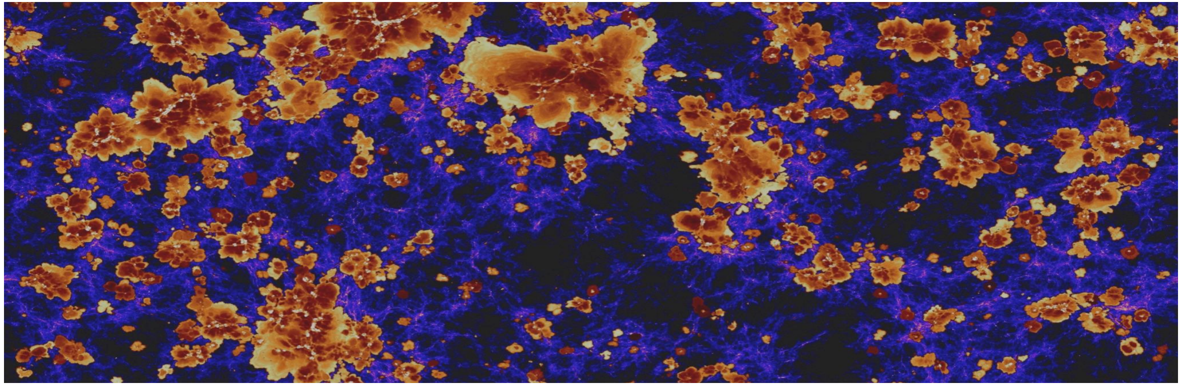

Joint constraints on reionization with the 21cm signal and kSZ

Joëlle-Marie Bégin
Princeton University

Observing the low-frequency sky with ALBATROS

THE 21 CM SIGNAL

WHAT IS IT?

THE 21 CM SIGNAL

WHAT IS IT?

WHY DO WE CARE?

THE 21 CM SIGNAL

WHAT IS IT?

WHY DO WE CARE?

WHAT DO WE KNOW?

The 21 cm signal: What is it?

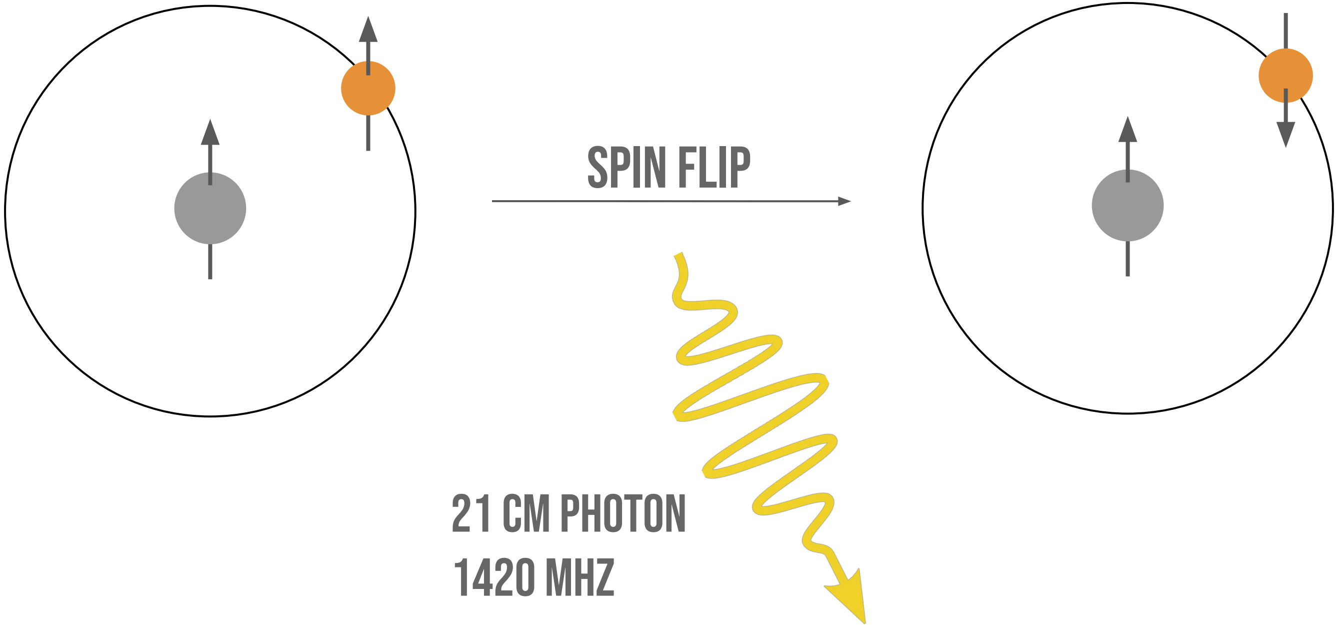

The 21 cm signal: What is it?

21cm differential brightness temperature

$$\delta T_b \propto x_{\mathrm{HI}} \frac{T_s - T_\gamma}{T_s}(1 + \delta_b)$$

The 21 cm signal: What is it?

$$\delta T_b \propto x_{\mathrm{HI}} \frac{T_s - T_\gamma}{T_s} (1 + \delta_b)$$

21cm differential brightness temperature (δT_b)

Fraction of neutral hydrogen (x_{HI})

21 cm spin temperature (T_s)

CMB temperature (T_γ)

Baryon density (δ_b)

The 21 cm signal: What is it?

Mapping fluctuations

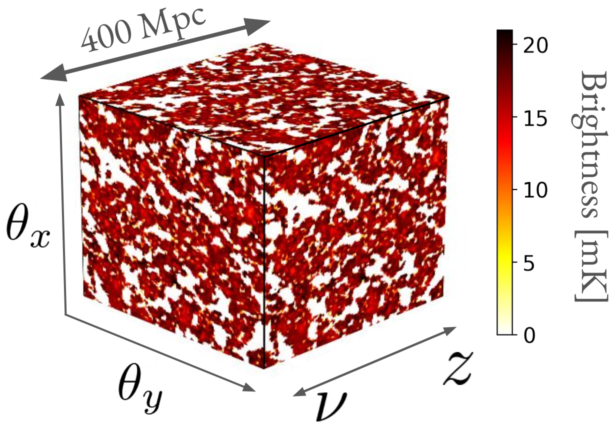

$$z = \frac{\nu_{\rm rest}}{\nu_{\rm obs}} - 1$$

HERA interferometer

The 21 cm signal: What is it?

Mapping fluctuations

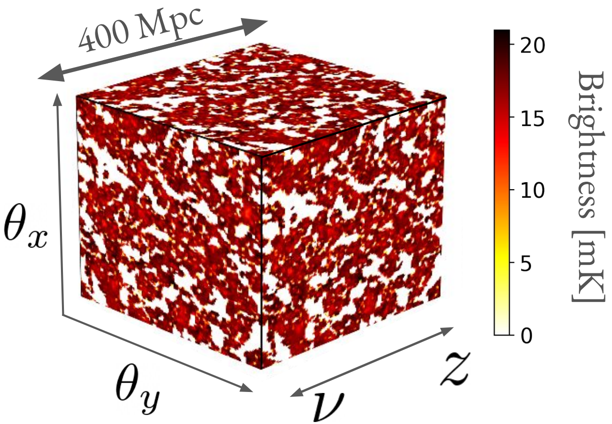

$$z = \frac{\nu_{\rm rest}}{\nu_{\rm obs}} - 1$$

The 21 cm signal: What is it?

Mapping fluctuations

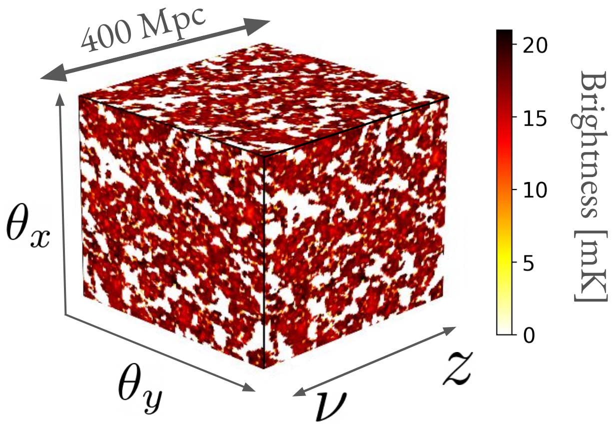

Spatial average

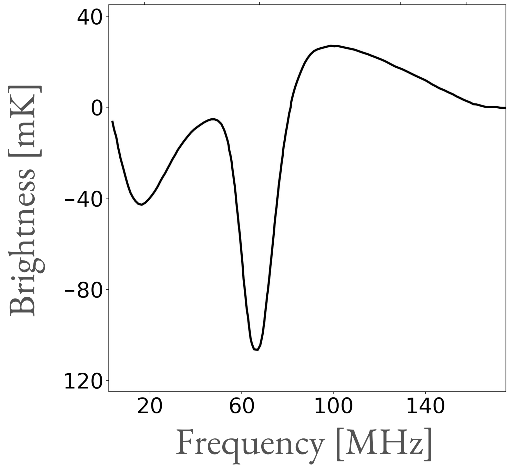

"Global signal"

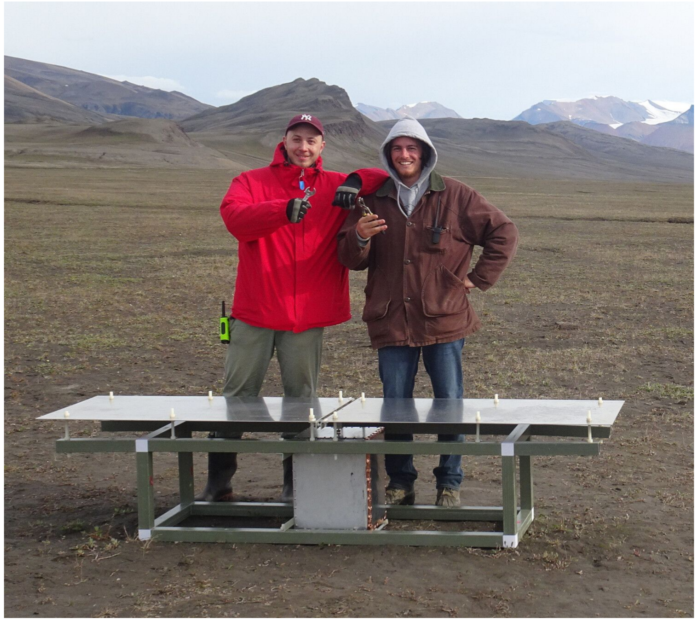

Ian Hendricksen and Vadym Vidulla at the McGill Arctic Research Station with the MIST global signal experiment

The 21 cm signal: What is it?

Mapping fluctuations

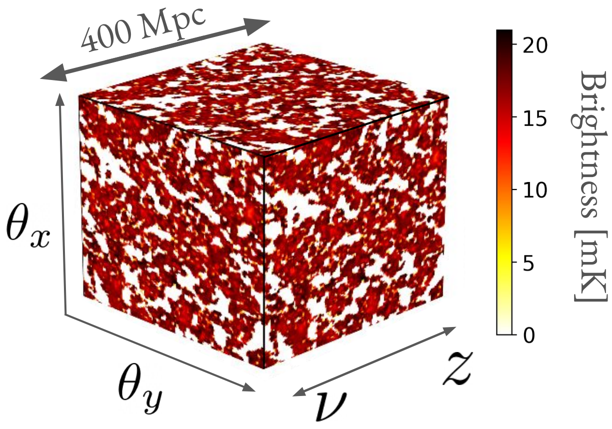

~

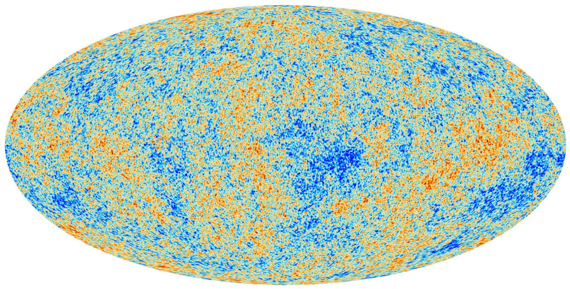

Spatial average

"Global signal"

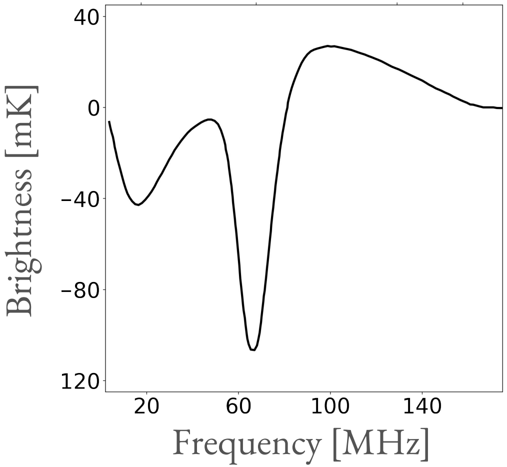

~

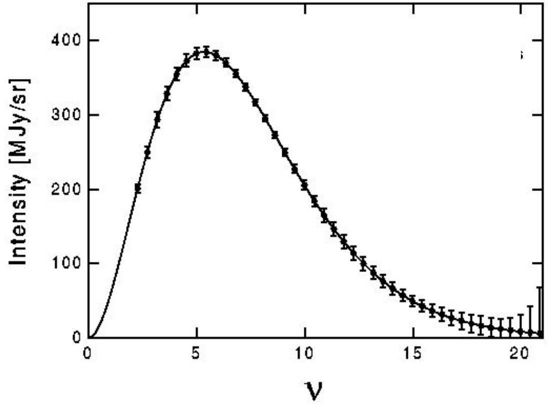

The 21 cm signal: What can we learn?

- Gives access to large volumes of the universe: tracer of LSS in 3D.

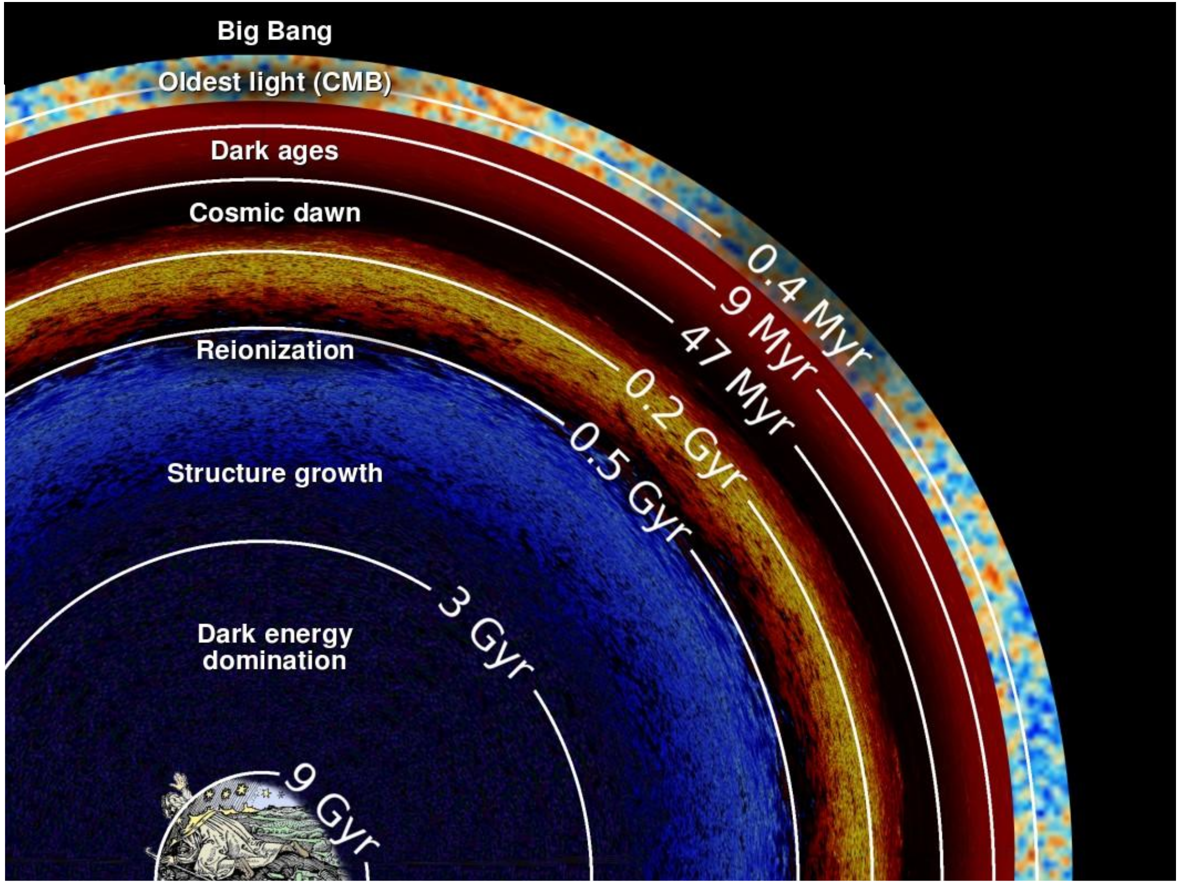

Image credits: Cynthia Chiang

The 21 cm signal: What can we learn?

- Gives access to large volumes of the universe: tracer of LSS in 3D.

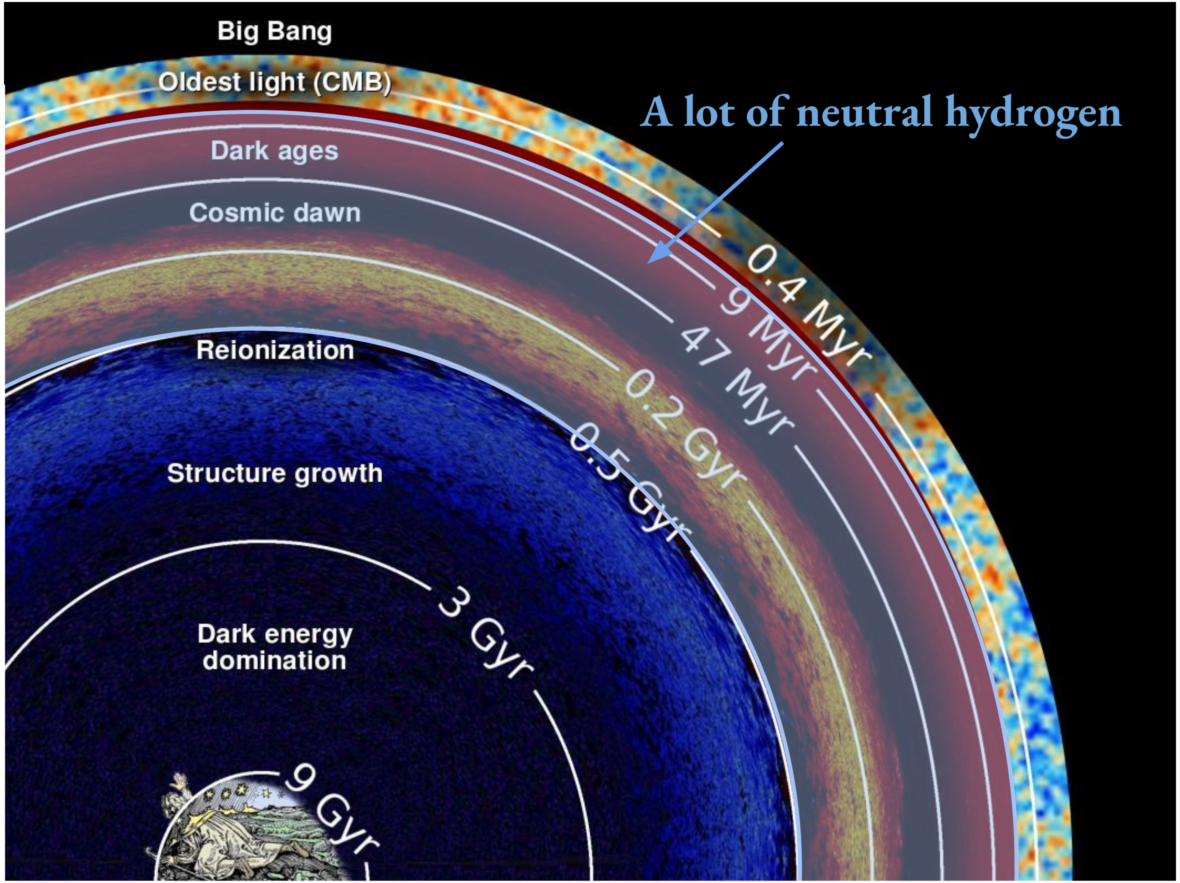

Image credits: Cynthia Chiang

The 21 cm signal: What can we learn?

- Gives access to large volumes of the universe: tracer of LSS in 3D.
- Improved constraints on the astrophysics of the early universe.
- Potential to break degeneracies in cosmological parameters.

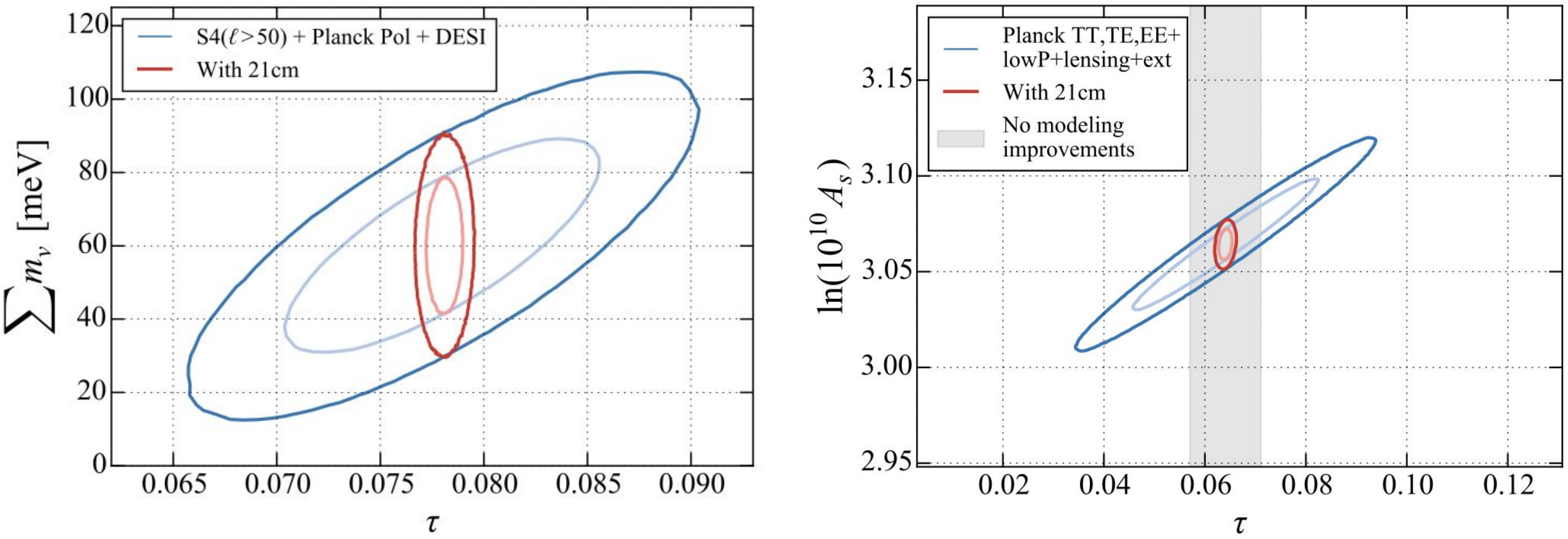

Liu et al 2016

The (global) 21 cm signal: What do we know?

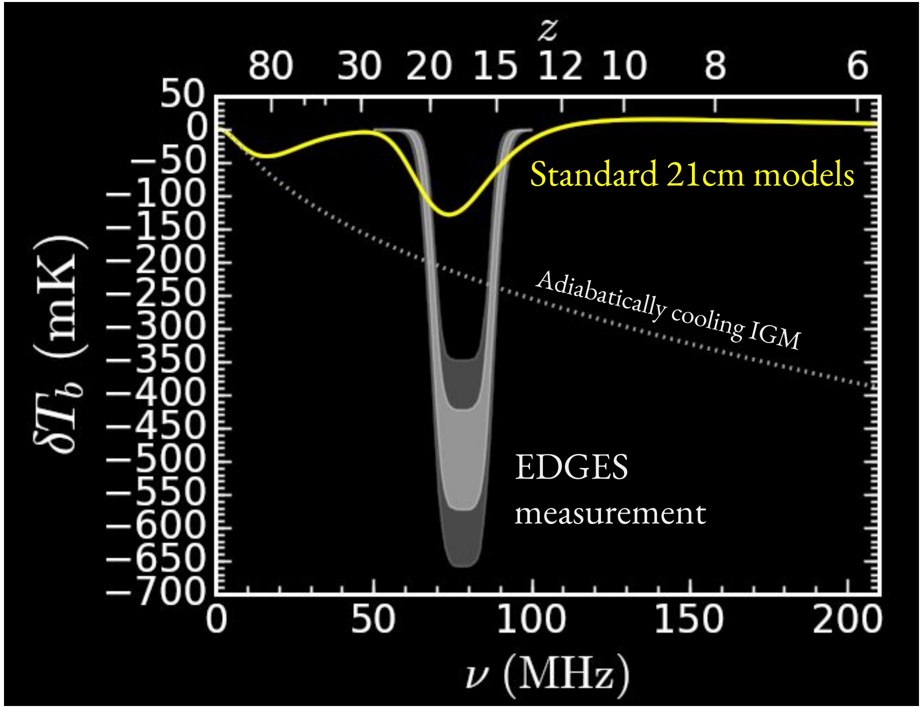

EDGES result (Bowman et al 2018)

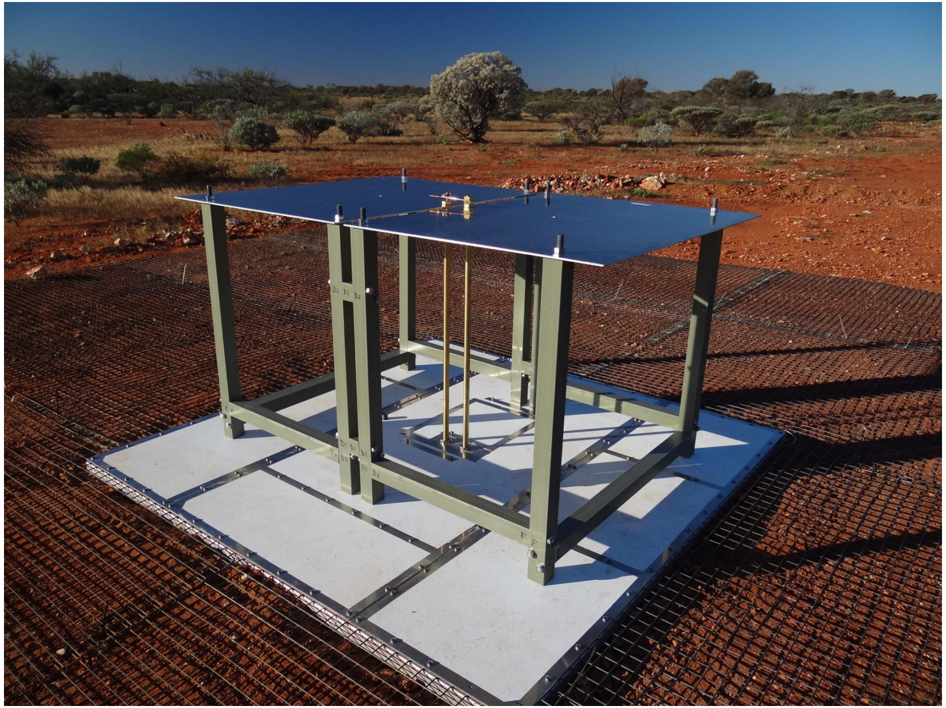

The (global) 21 cm signal: What do we know?

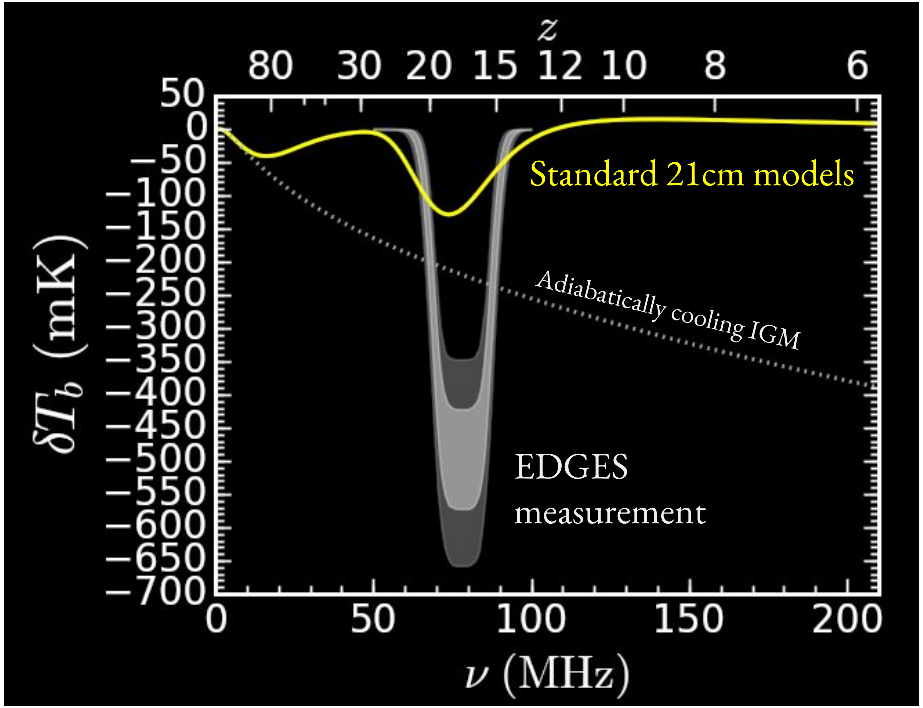

EDGES result (Bowman et al 2018)

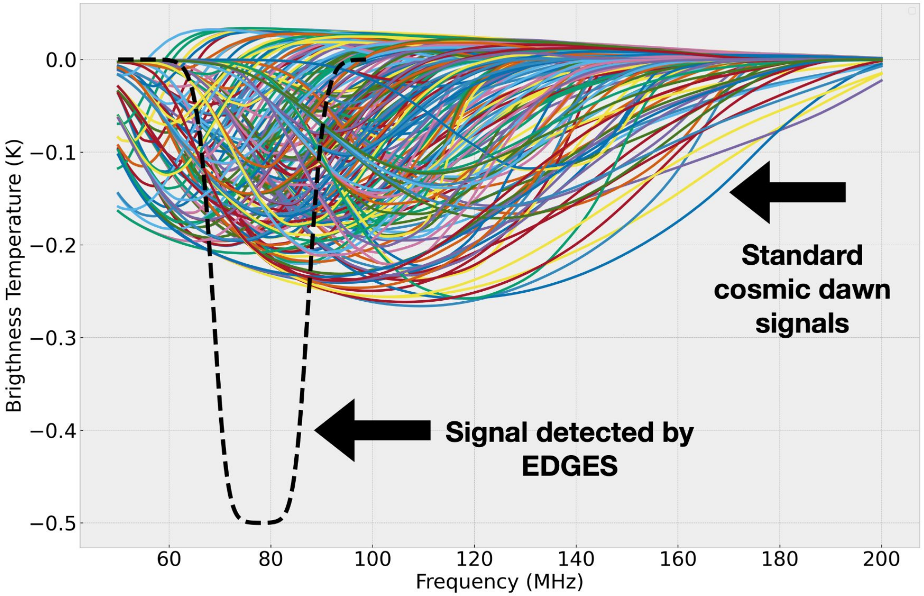

Saurabh Singh (2022)

The (global) 21 cm signal: What do we know?

Exotic baryon-DM interactions, DM decay?
(1803.06698, 1802.10577, 1802.10094)

Synchrotron radiation from black holes?
(1803.01815)

Unpredicted high z radio excess?
(1802.07432)

Systematics

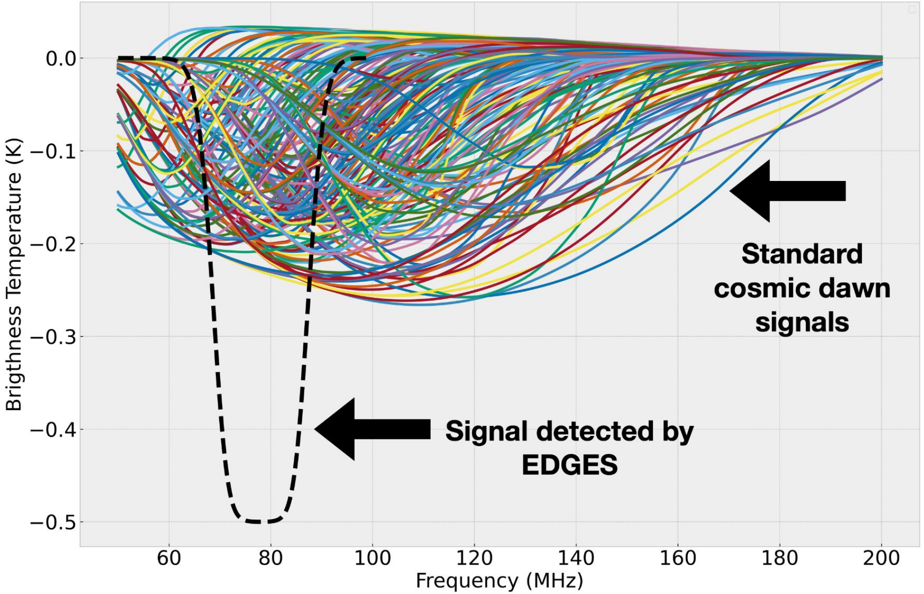

Saurabh Singh (2022)

The (global) 21 cm signal: What do we know?

SARAS experiment: follow up to EDGES

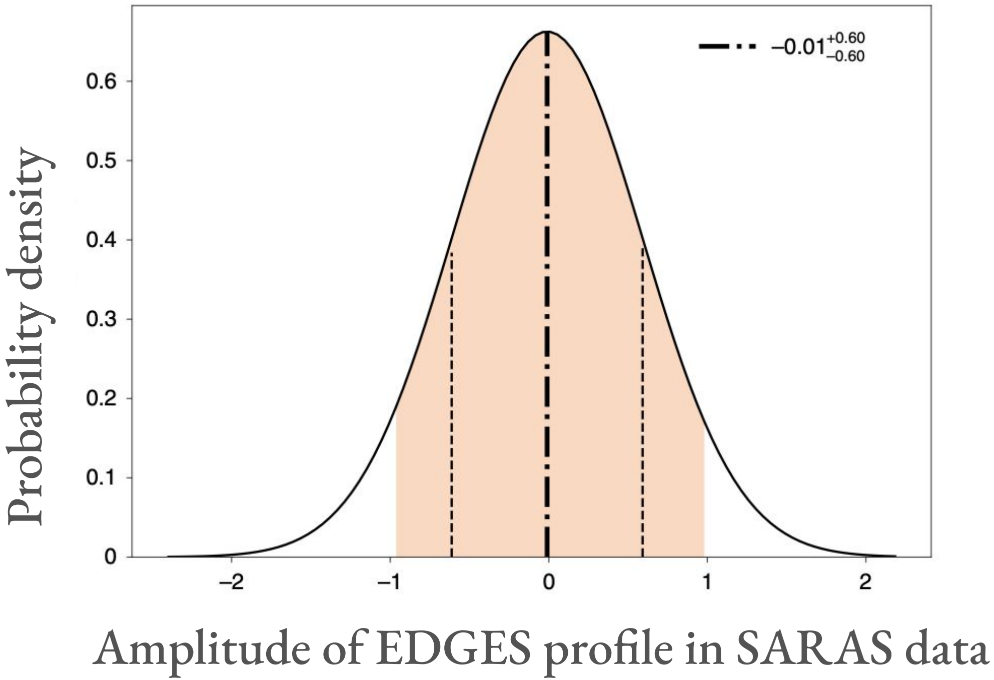

The (global) 21 cm signal: What do we know?

SARAS experiment: follow up to EDGES

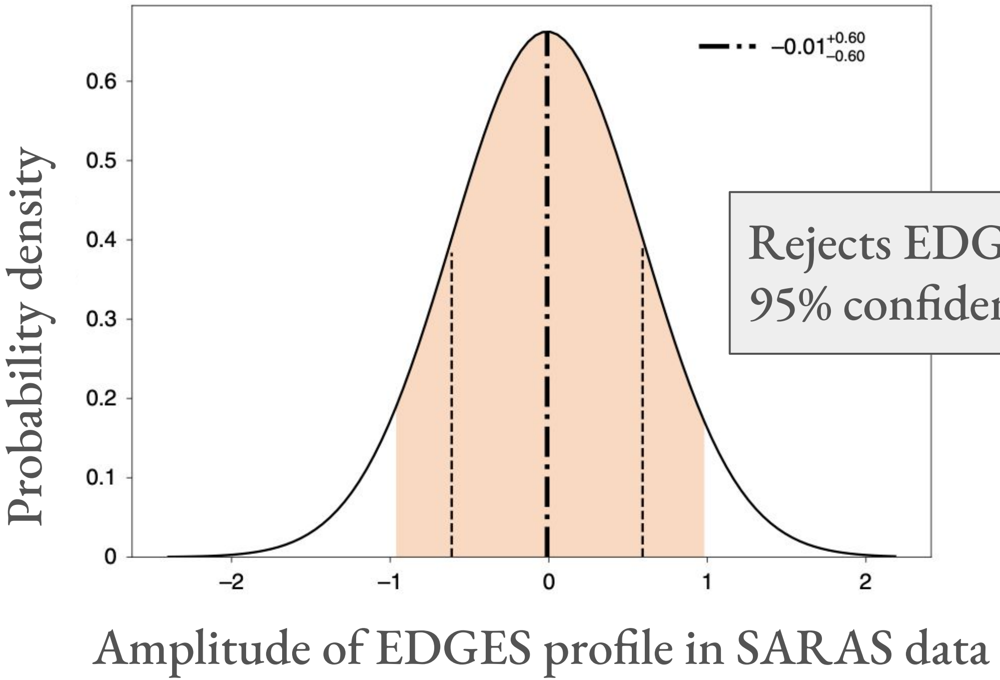

Rejects EDGES profile at 95% confidence.

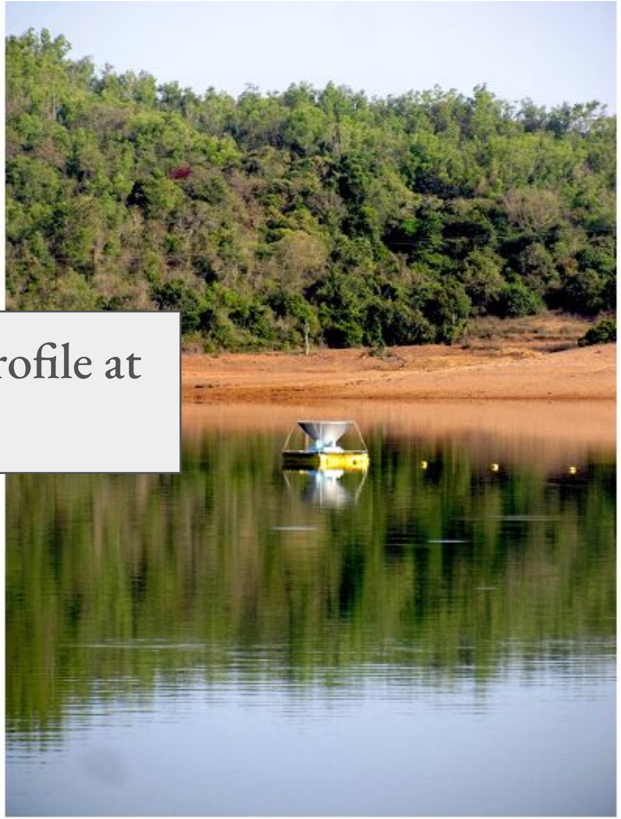

WHAT IS THE 21 CM SIGNAL?

Redshifted emission from neutral hydrogen's hyperfine transition.

WHAT CAN WE LEARN FROM IT?

Evolution of large scale structure for $z > 6$.
Early universe astrophysics.
Potentially break degeneracies in cosmological parameters.

WHAT DO WE KNOW?

One detection of the global signal at 80 MHz + follow up non-detection.

Constraining reionization with the global 21cm signal and kSZ

In collaboration with Adrian
Liu and Adelie Gorce

The ionization history

$$\tau \propto \int dz \, x_{\mathrm{HII}}(z)$$

Fraction of ionized hydrogen

The ionization history

- Some bounds on midpoint, end, and duration.

Monsalve et al, 2017

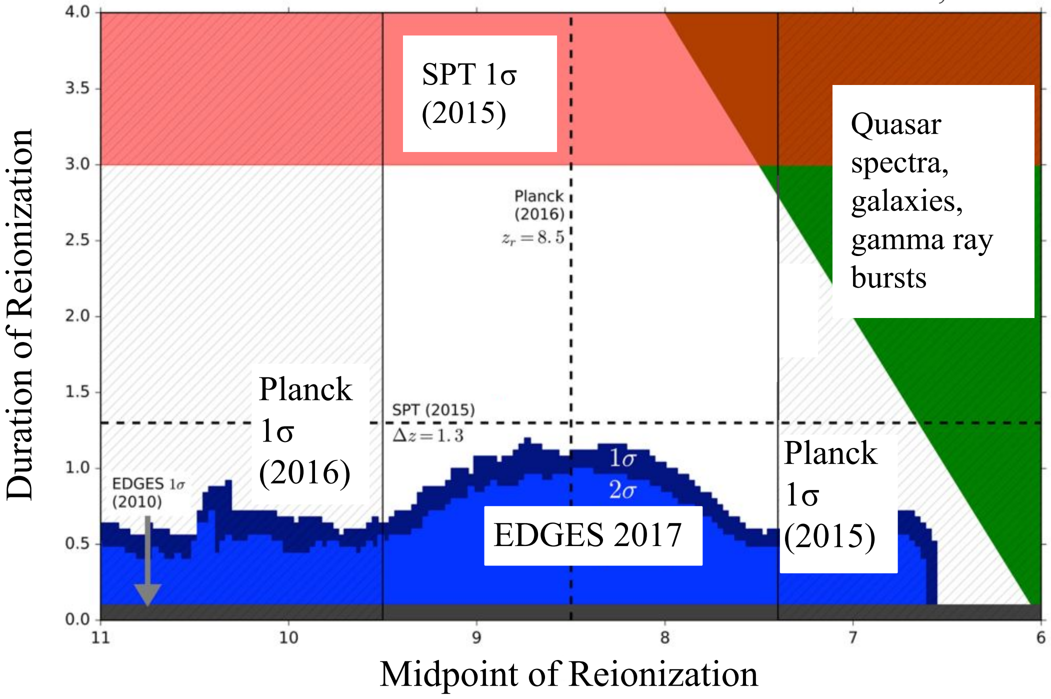

The ionization history

- Some bounds on midpoint, end, and duration.
- Few limits on precise shape.

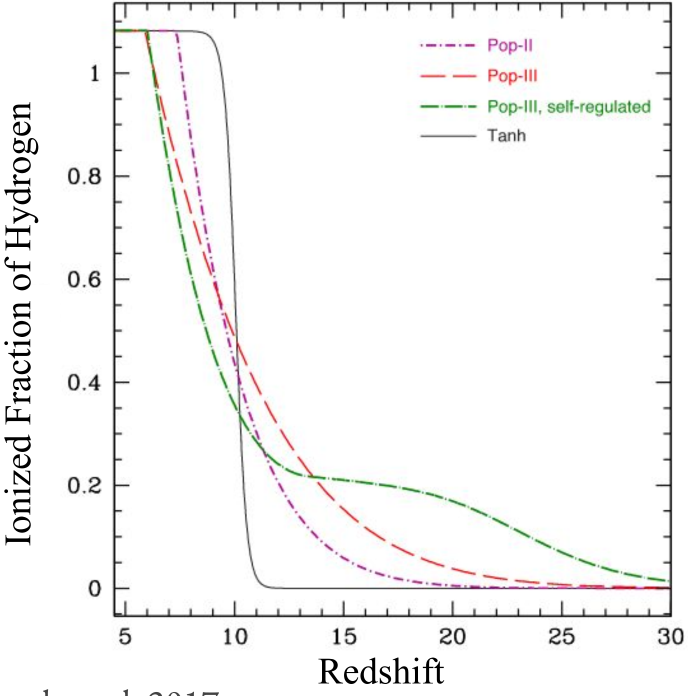

Miranda et al, 2017

Monsalve et al, 2017

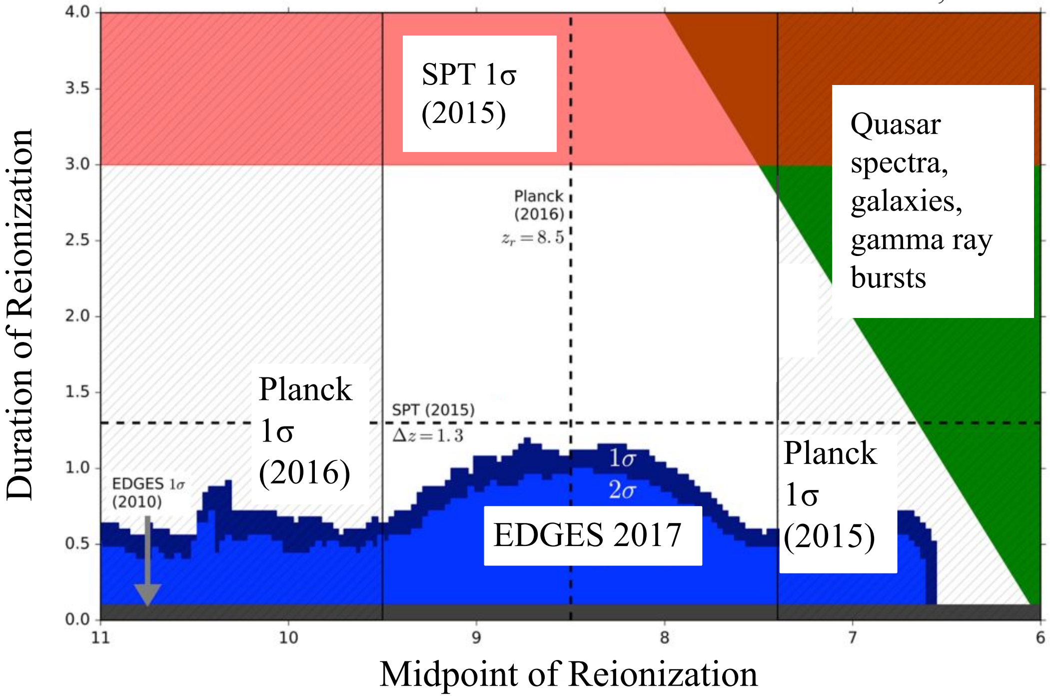

The global 21cm signal as a probe of reionization

- During reionization, the global signal closely tracks the ionization history

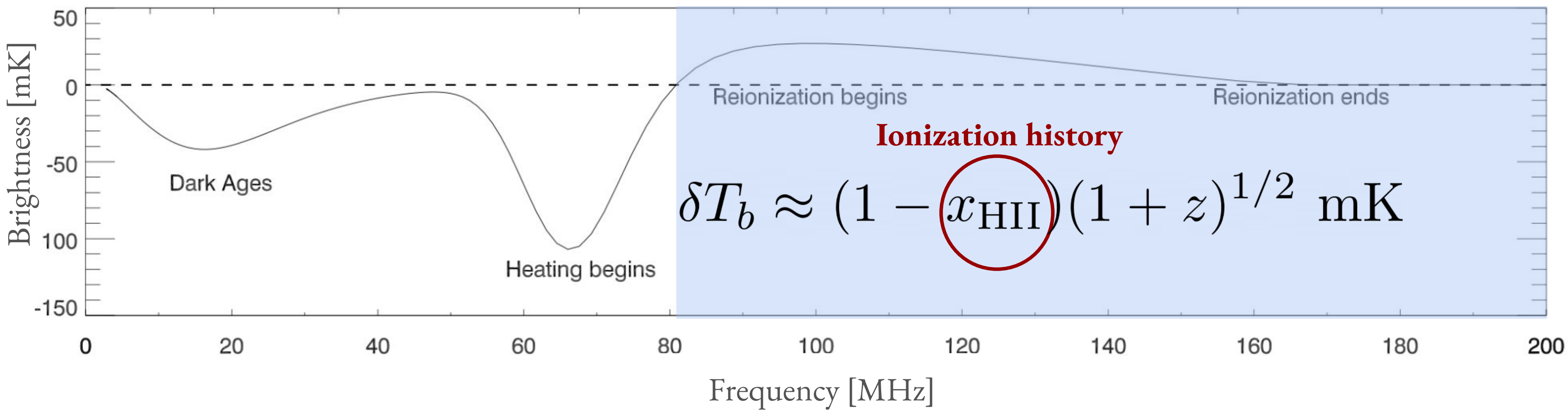

Pritchard and Loeb 2012

The global 21cm signal as a probe of reionization

- During reionization, the global signal closely tracks the ionization history
- The global signal is **most sensitive to rapidly evolving reionization histories** due to spectrally smooth foregrounds

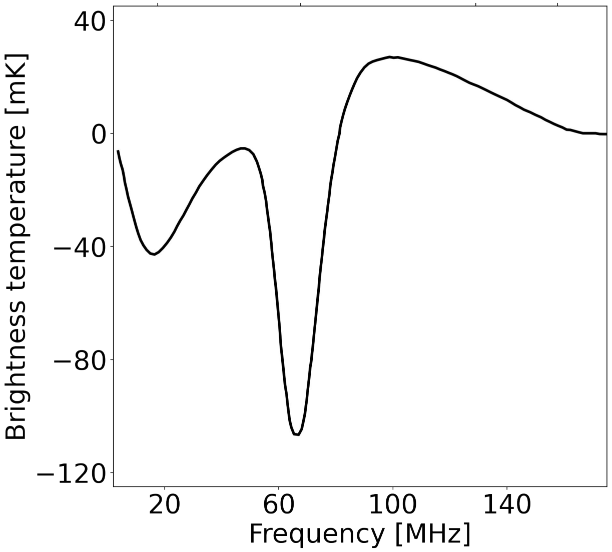

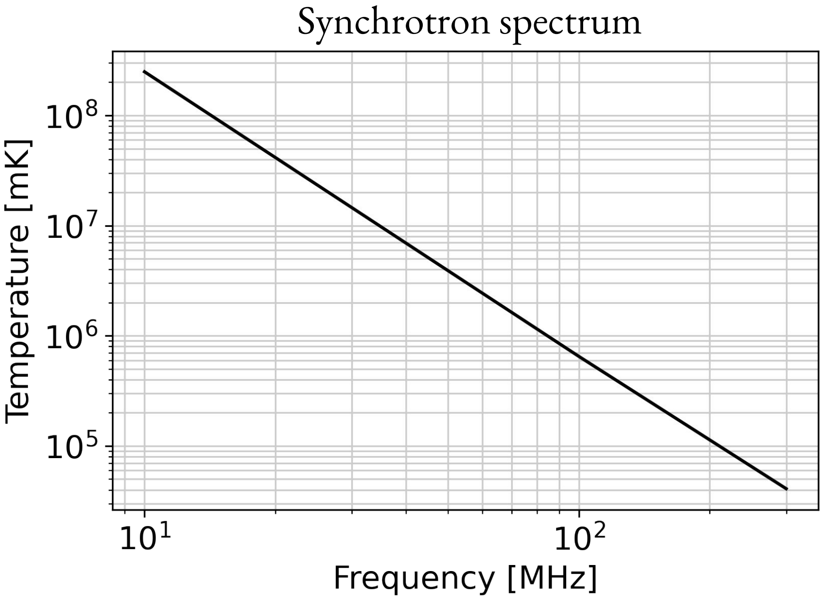

The kinetic Sunyaev-Zeldovich effect (kSZ)

- CMB photons scattering off of energetic electrons with bulk relative velocity
- Power spectrum changes with midpoint, duration, morphology of reionization

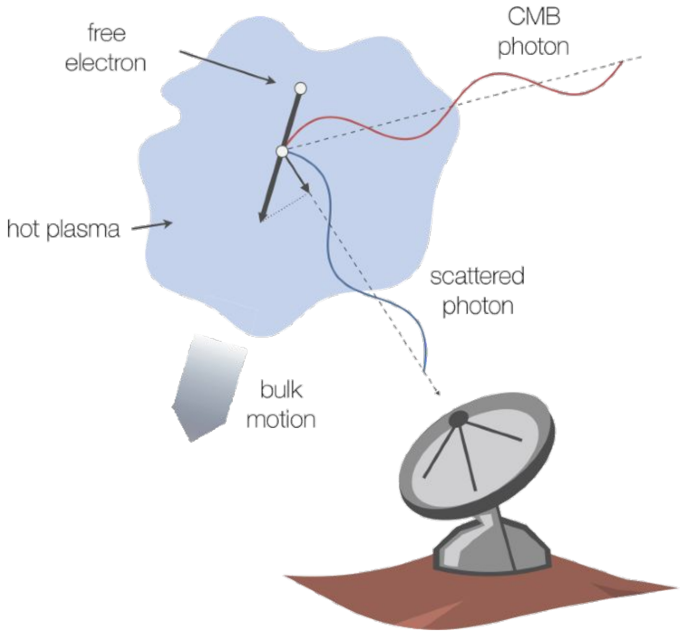

Mroczskowski et al, 2019

The kinetic Sunyaev-Zeldovich effect (kSZ)

- CMB photons scattering off of energetic electrons with bulk relative velocity
- Power spectrum changes with midpoint, duration, morphology of reionization

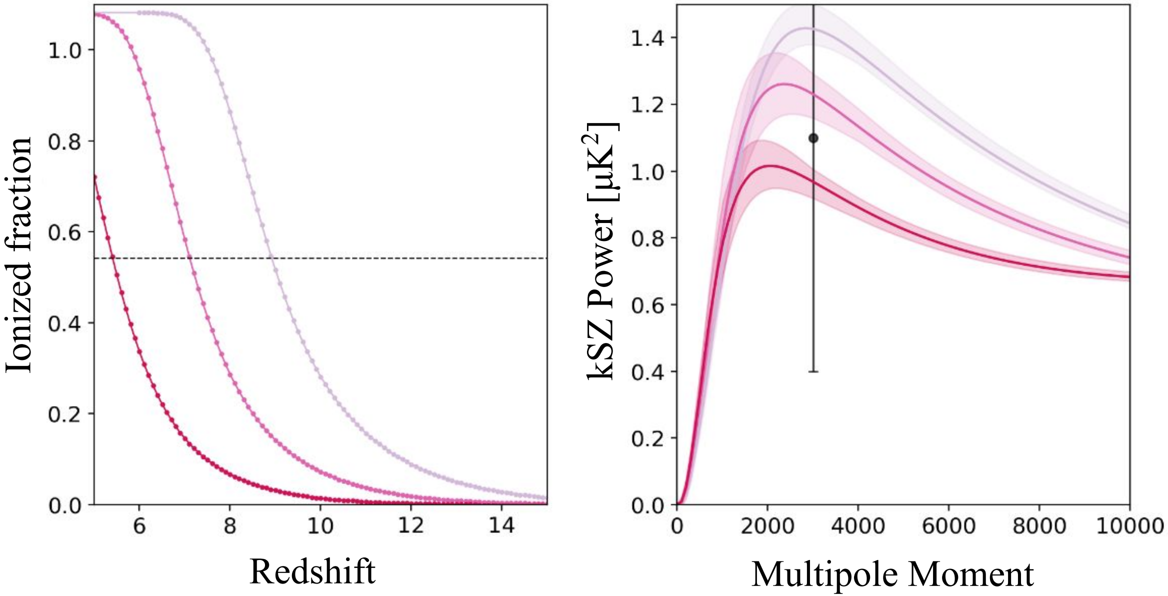

Gorce et al, 2020

The global signal is sensitive to **rapidly evolving** ionization histories, the kSZ to **extended** ionization histories.

The Karhunen-Loève (KL) Transform

- A transformation whose eigenvalues represent the ratio of two signals.
- Familiar example: signal-to-noise analysis and data compression.

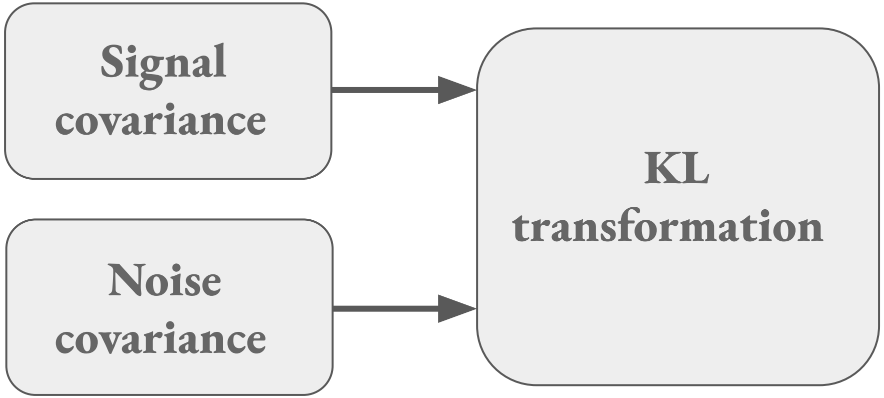

The Karhunen-Loève (KL) Transform

- A transformation whose eigenvalues represent the ratio of two signals.
- Familiar example: signal-to-noise analysis and data compression.

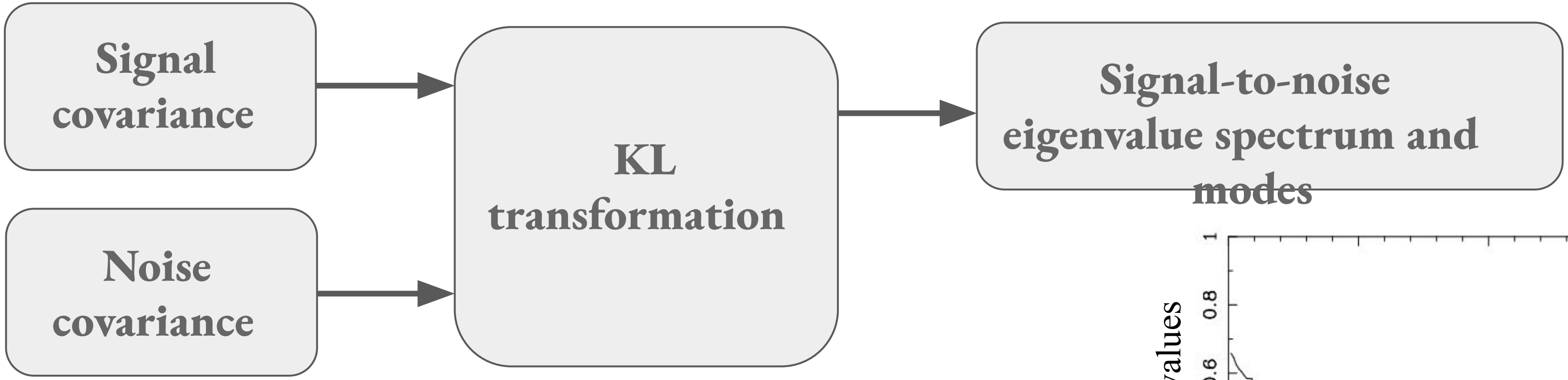

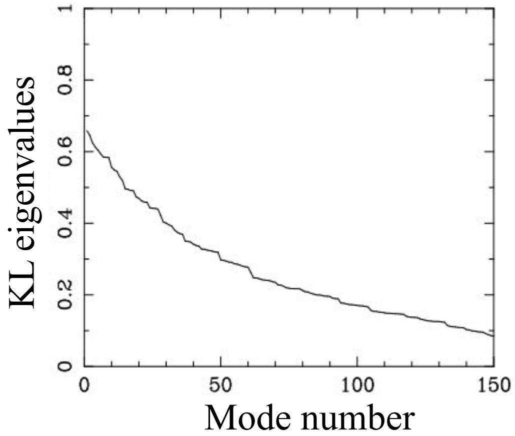

Tegmark, Taylor & Heavens (1996)

The Karhunen-Loève (KL) Transform

- A transformation whose eigenvalues represent the ratio of two signals.
- Familiar example: signal-to-noise analysis and data compression.

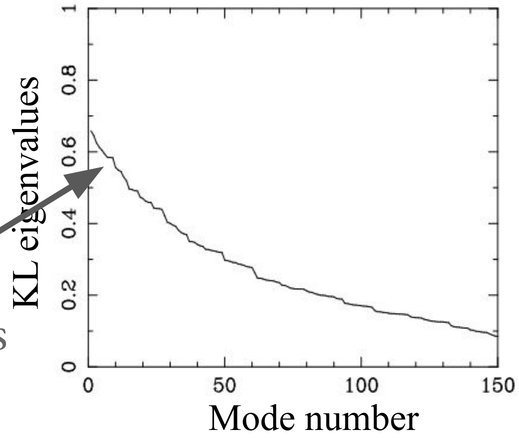

High signal-to-noise eigenvalues

Tegmark, Taylor & Heavens (1996)

The Karhunen-Loève (KL) Transform

- In our case: kSZ-to-21cm analysis
- Fisher matrices computed with analytic 21cm and kSZ models

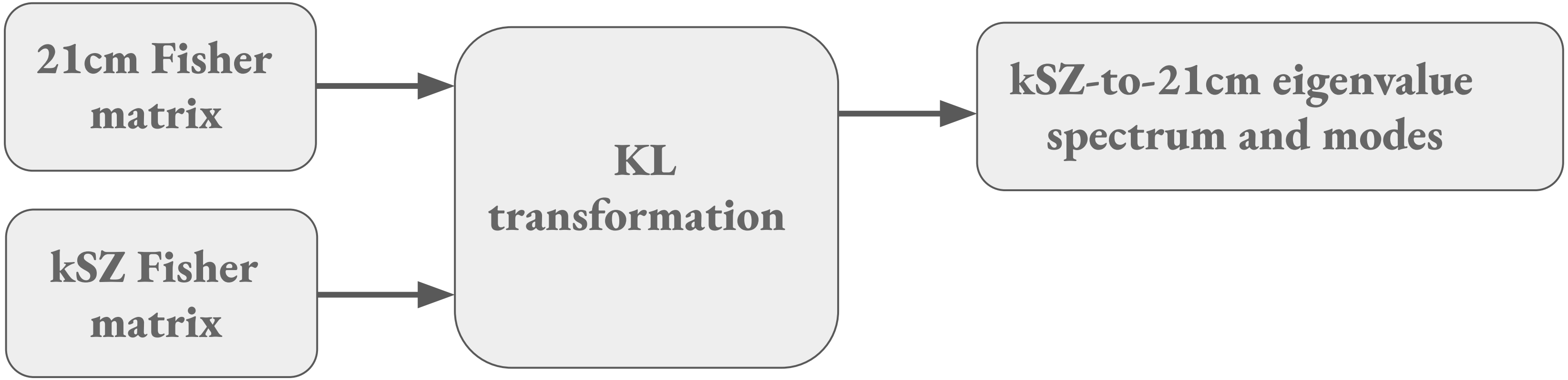

$$\mathbf{F}_{\mathrm{kSZ}}\mathbf{v} = \lambda \mathbf{F}_{21}\mathbf{v}$$

21cm-to-kSZ eigenvalues and modes

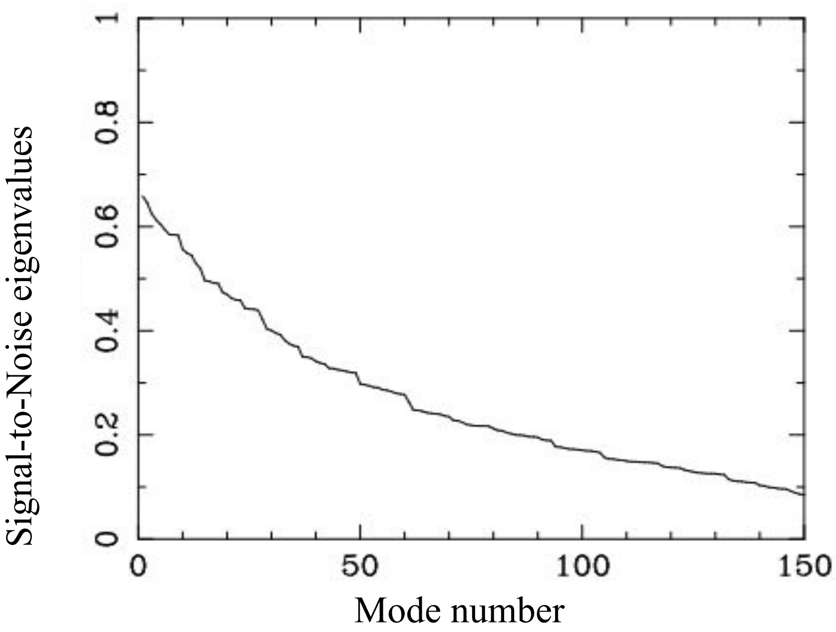

Tegmark, Taylor & Heavens (1996)

21cm-to-kSZ eigenvalues and modes

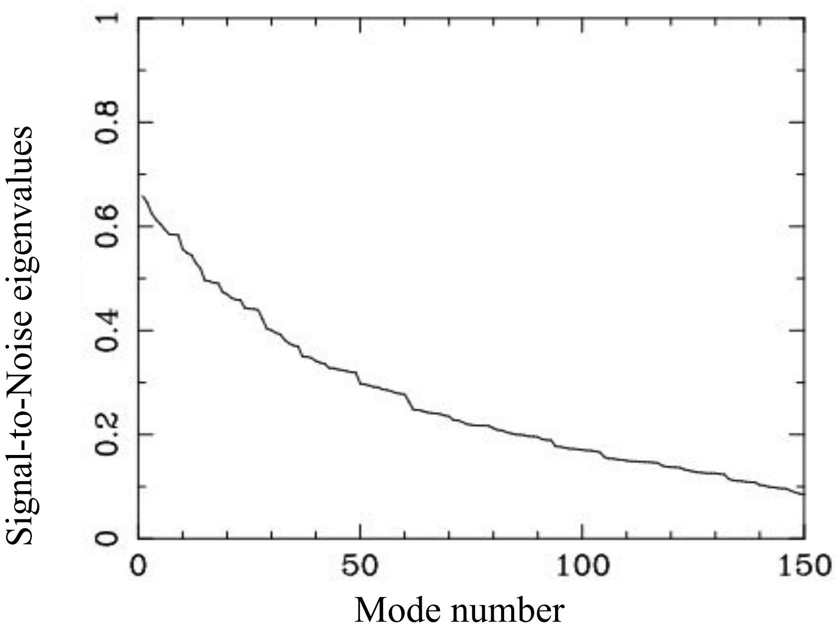

Tegmark, Taylor & Heavens (1996)

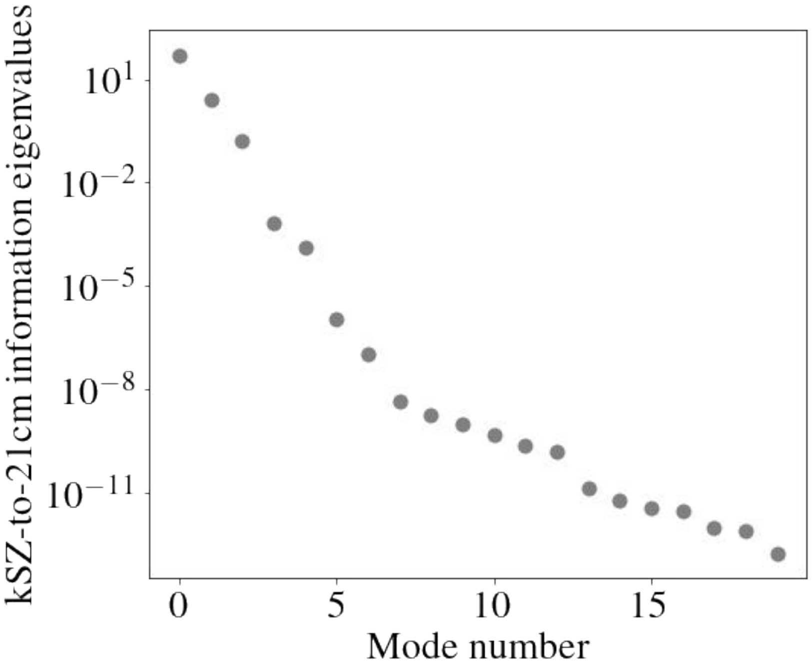

Begin, Liu & Gorce

21cm-to-kSZ eigenvalues and modes

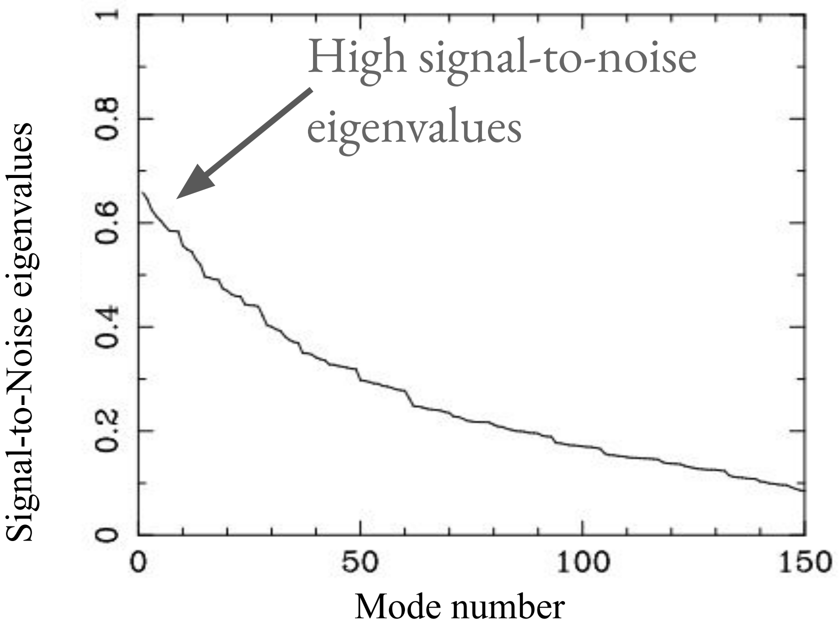

Tegmark, Taylor & Heavens (1996)

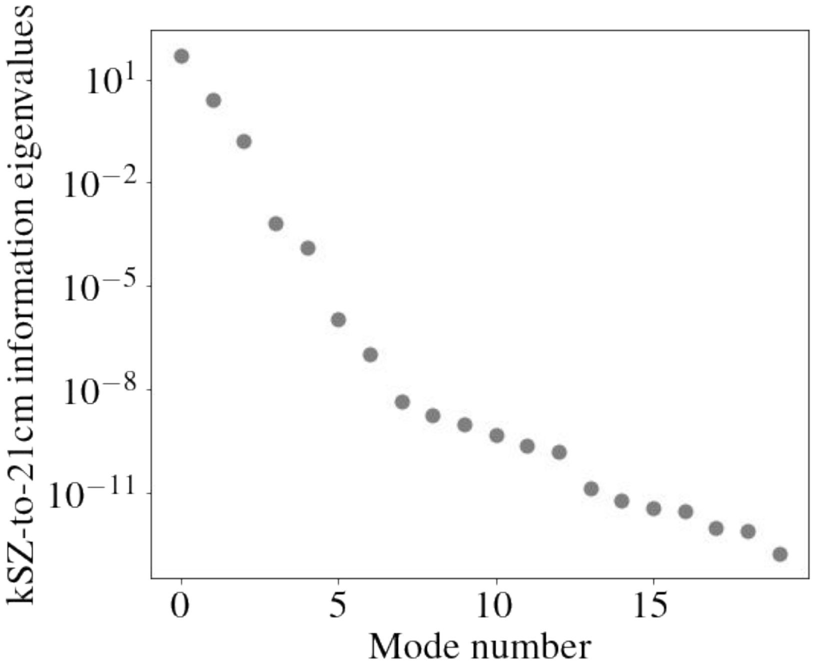

Begin, Liu & Gorce

21cm-to-kSZ eigenvalues and modes

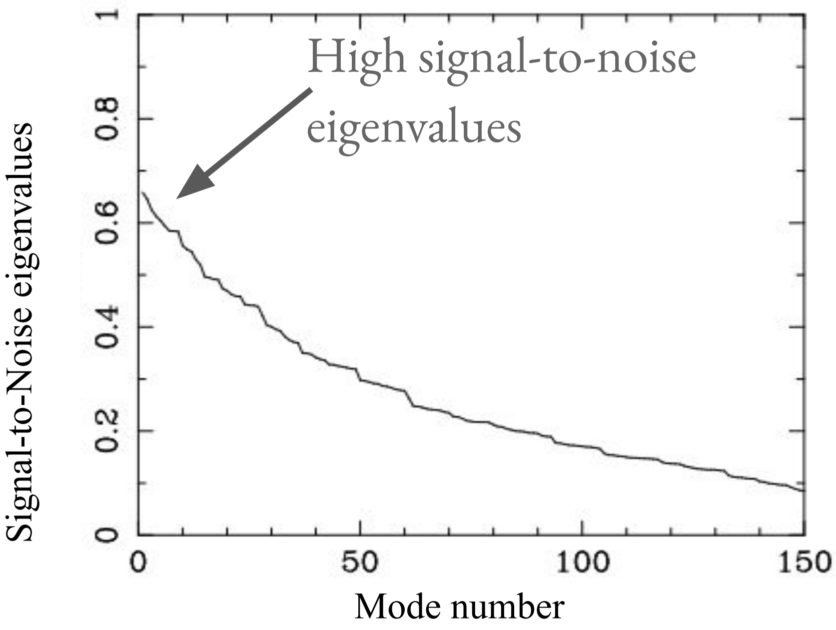

Tegmark, Taylor & Heavens (1996)

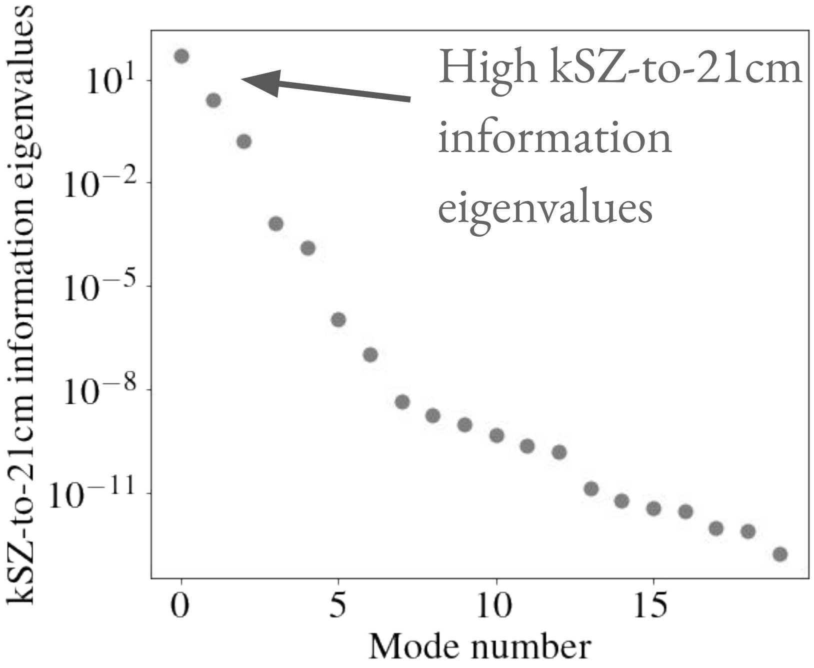

Begin, Liu & Gorce

21cm-to-kSZ eigenvalues and modes

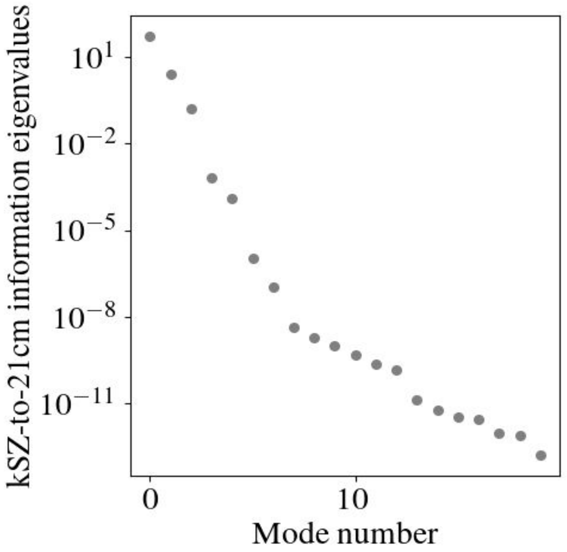

21cm-to-kSZ eigenvalues and modes

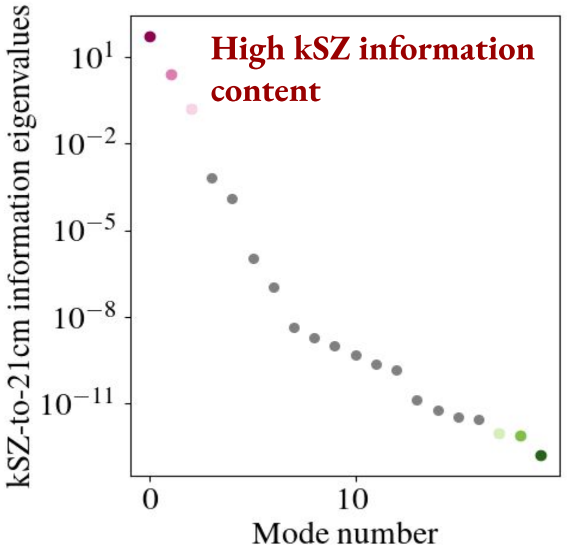

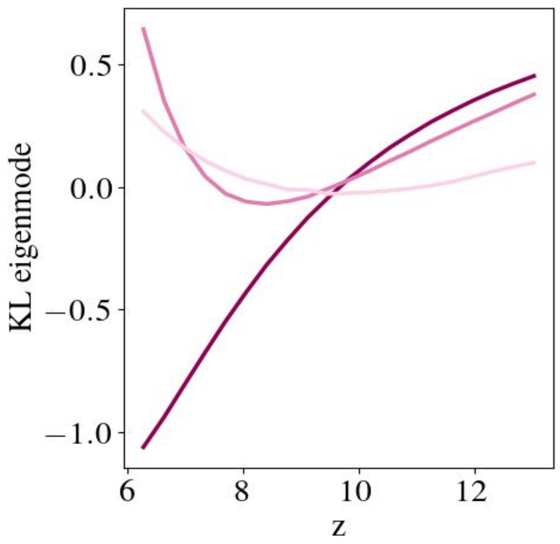

21cm-to-kSZ eigenvalues and modes

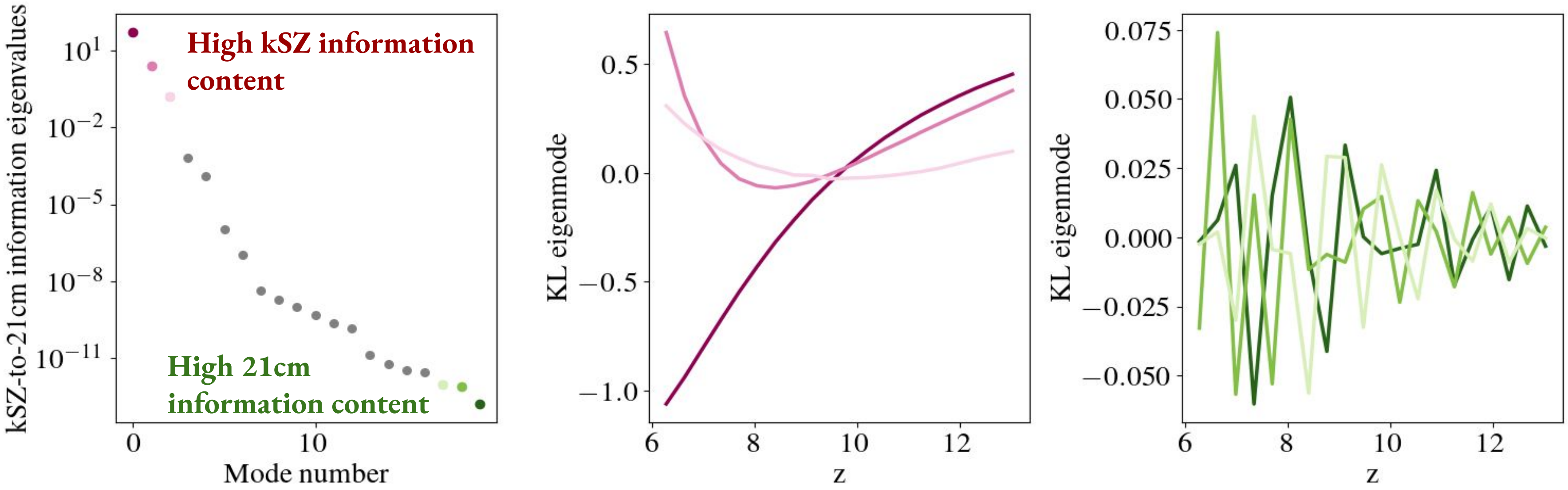

21cm-to-kSZ eigenvalues and modes

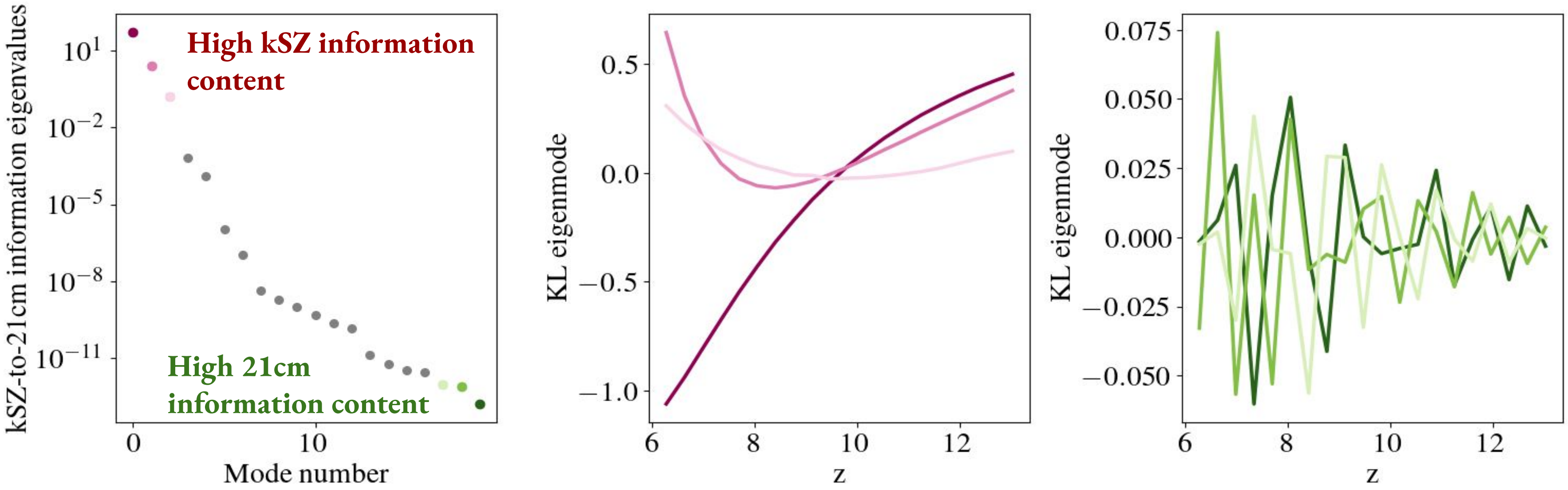

$$x_{HI}(z) = \sum_i a_i \phi_i(z)$$

KL modes

21cm-to-kSZ eigenvalues and modes

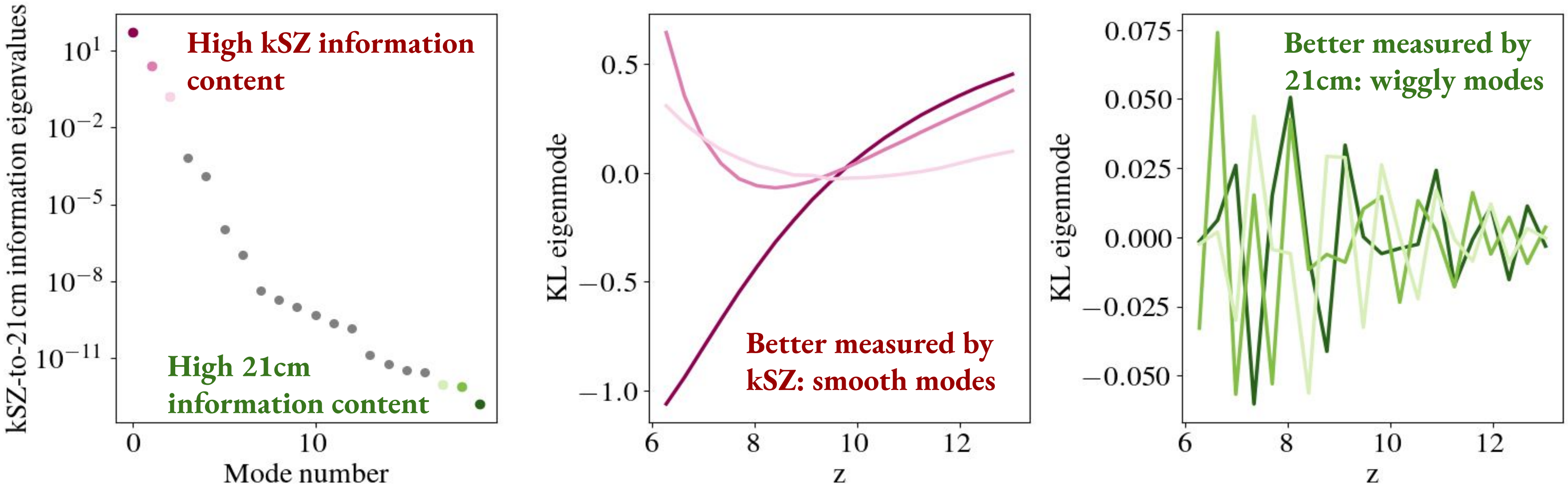

$$x_{HI}(z) = \sum_i a_i \phi_i(z)$$

KL modes

Constraining reionization: linear least squares

Measurement of KL amplitudes by **kSZ**

$$\boxed{\mathbf{y}} = \mathbf{A}\boxed{\mathbf{x}} + \mathbf{n}$$

"True" ionization history

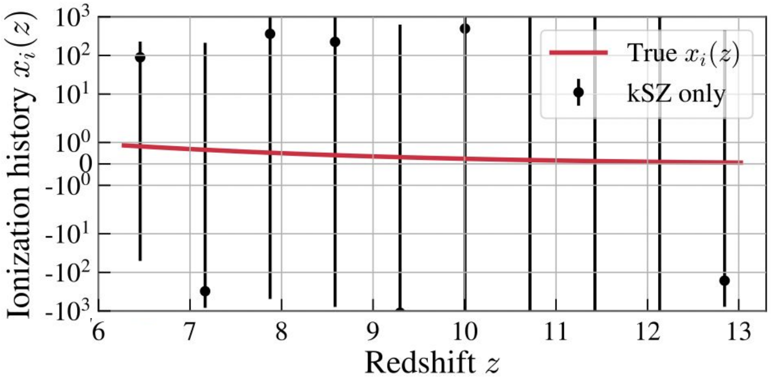

$$\hat{\mathbf{x}} = (\mathbf{A}^T\mathbf{N}^{-1}\mathbf{A})^{-1}\mathbf{A}^T\mathbf{N}^{-1}\mathbf{y}$$

Constraining reionization: linear least squares

Measurement of KL amplitudes by **21cm**

$$\mathbf{y} = \mathbf{A}\mathbf{x} + \mathbf{n}$$

"True" ionization history

$$\hat{\mathbf{x}} = (\mathbf{A}^T\mathbf{N}^{-1}\mathbf{A})^{-1}\mathbf{A}^T\mathbf{N}^{-1}\mathbf{y}$$

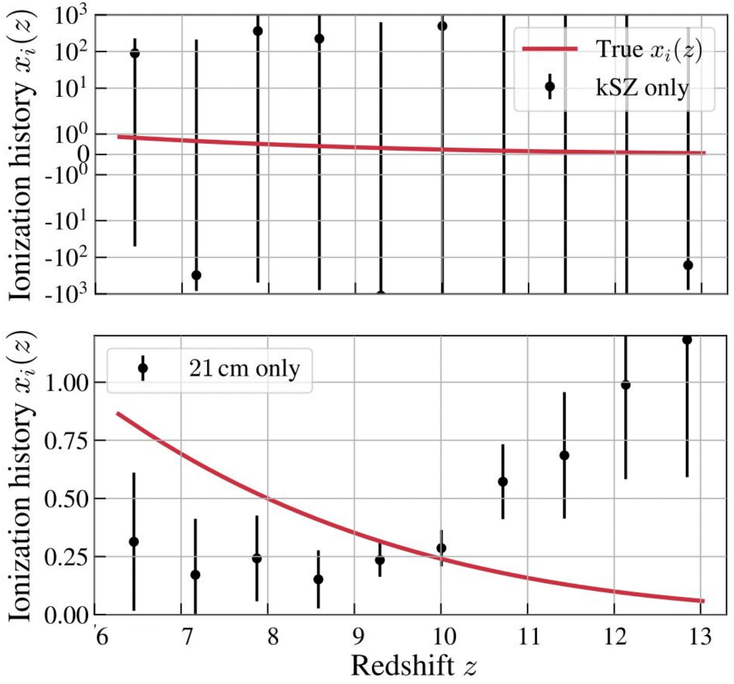

Constraining reionization: linear least squares

Concatenated 21cm and kSZ measurements

$$\boxed{\mathbf{y}} = \mathbf{A}\boxed{\mathbf{x}} + \mathbf{n}$$

"True" ionization history

$$\hat{\mathbf{x}} = (\mathbf{A}^T\mathbf{N}^{-1}\mathbf{A})^{-1}\mathbf{A}^T\mathbf{N}^{-1}\mathbf{y}$$

Assumes no parametrization of the ionization history.

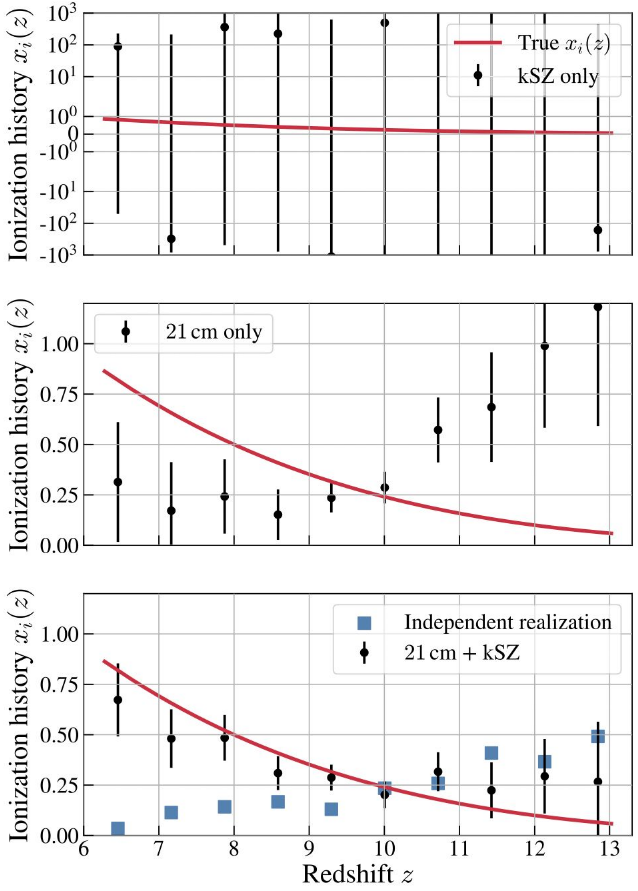

Constraining reionization: linear least squares

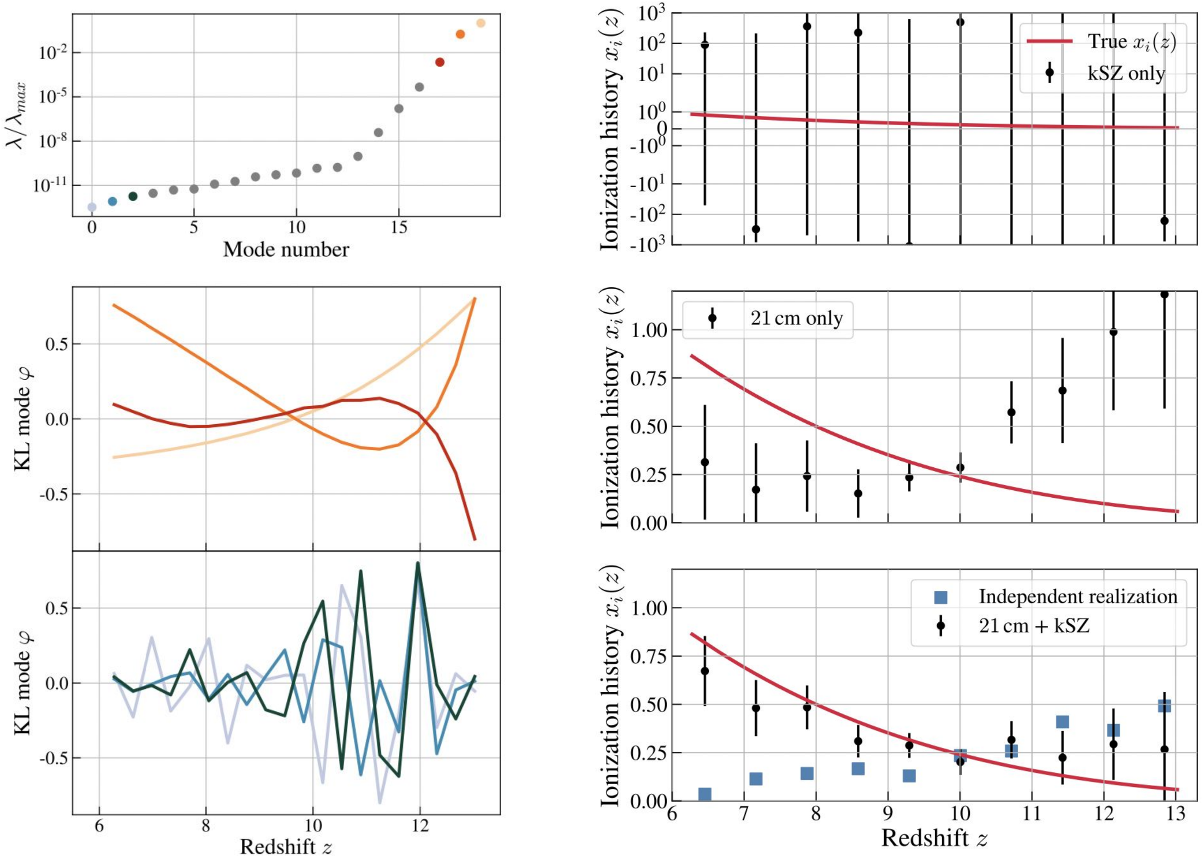

Constraining reionization: Bayesian methods

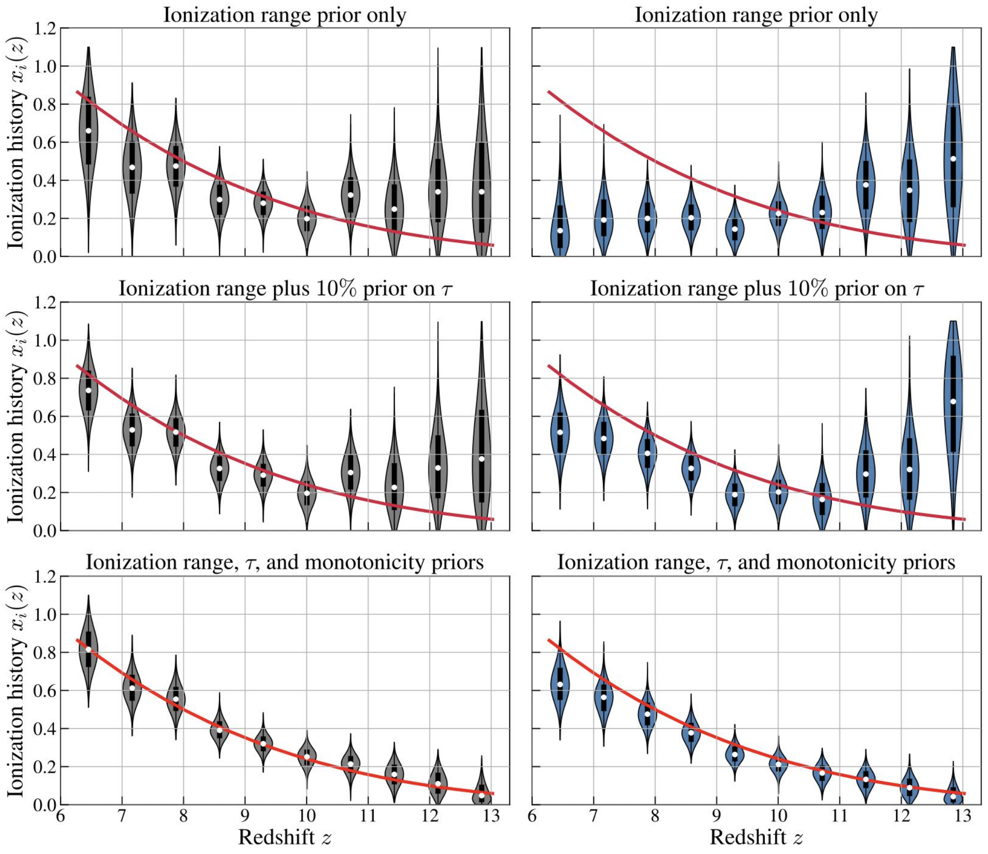

Summary

- The Karhunen-Loève basis highlights the complementary relation between the kSZ and 21cm global signal.
- Combining these two gives us access to modes of the ionization history that each probe in isolation does not constrain.
- KL basis facilitates detection of systematic by harnessing “overlap modes”.

  (Begin, Liu & Gorce: 2112.06933)
- This is a general framework that can be **extended to any two probes**.

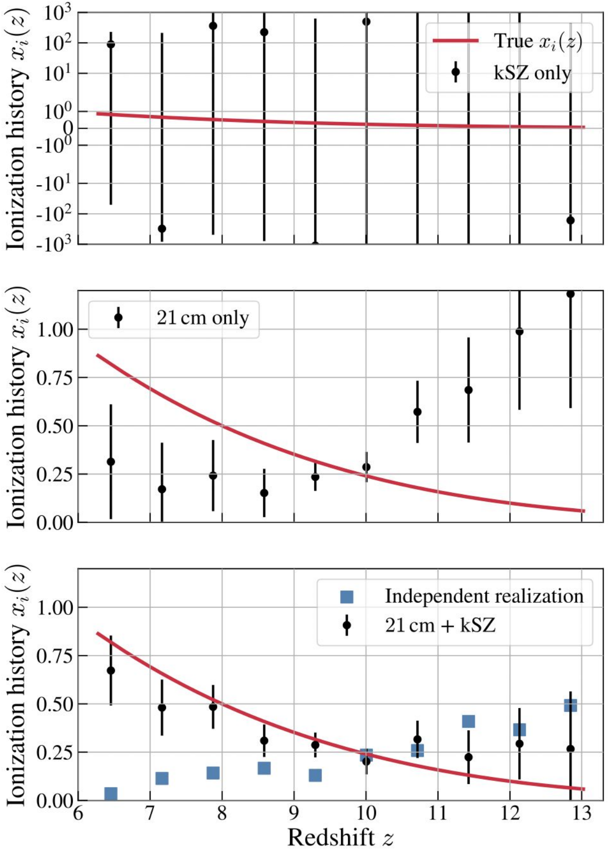

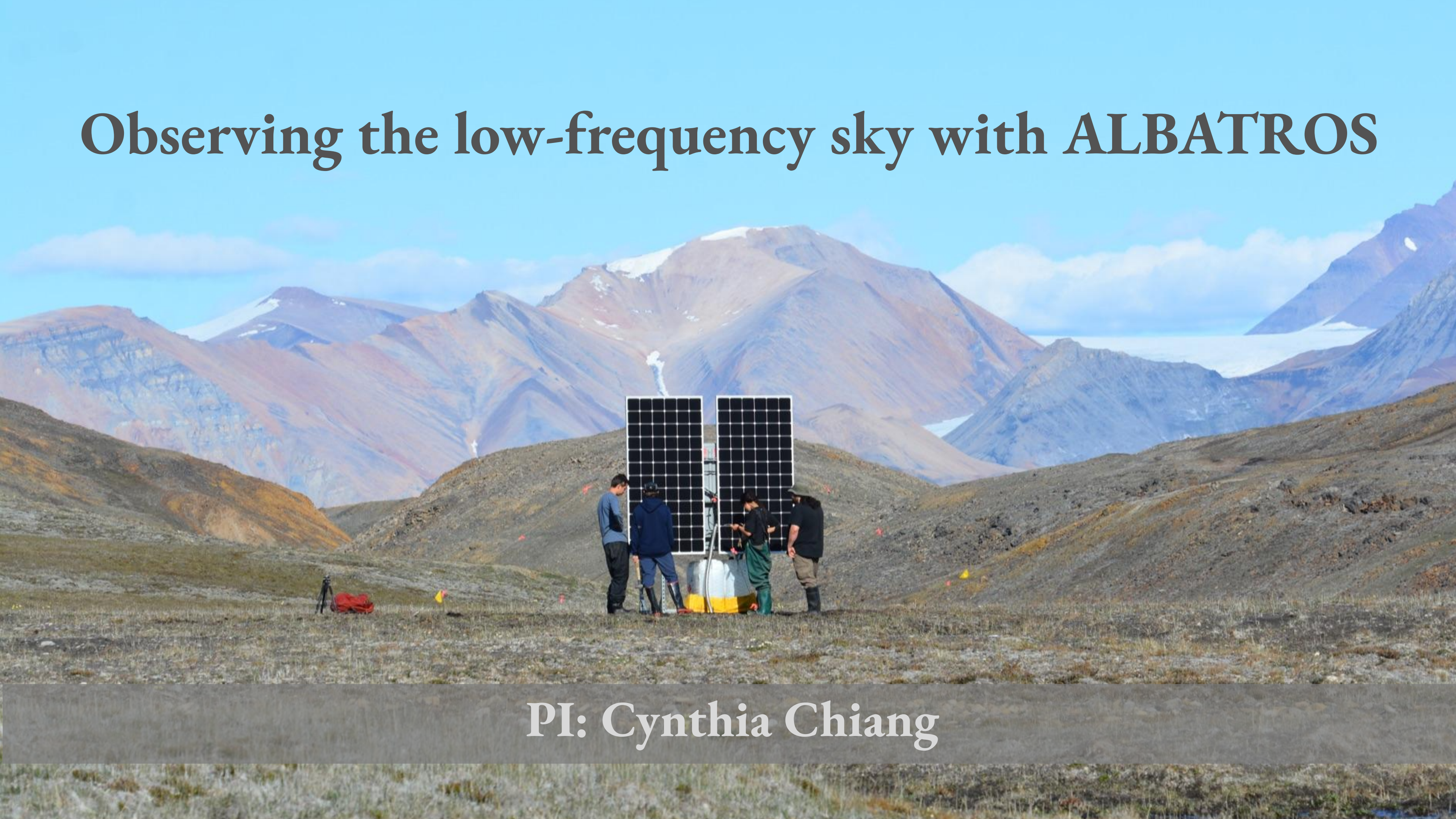
Observing the low-frequency sky with ALBATROS
PI: Cynthia Chiang

ALBATROS Overview

- The **A**rray of **L**ong **B**aseline **A**ntennas for **T**aking **R**adio **O**bservations from the **S**ub-antarctic/**S**eventy-ninth parallel
- Goal: map the sky below 30 MHz
- Remote locations to minimize RFI
- Autonomous antenna stations with ~10 km baselines

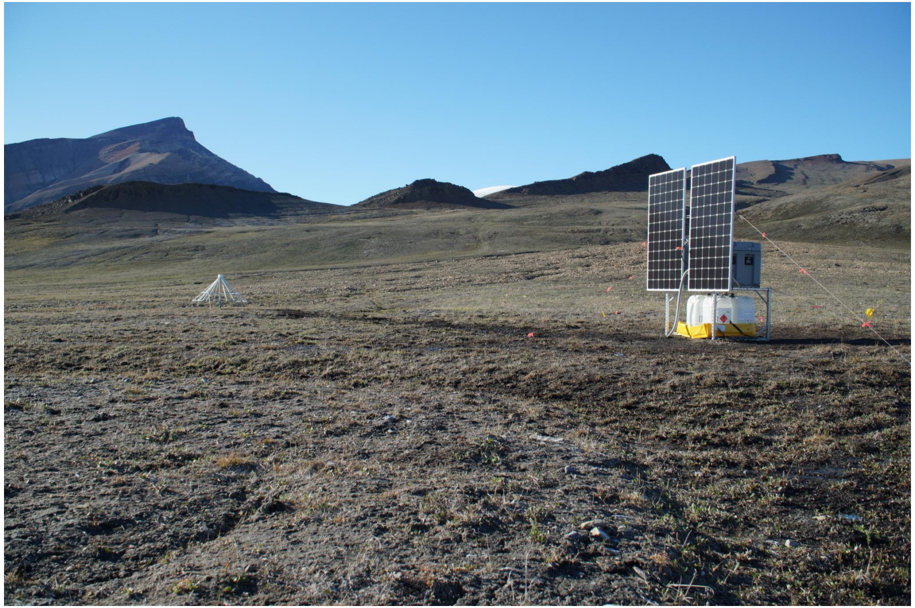

ALBATROS Overview

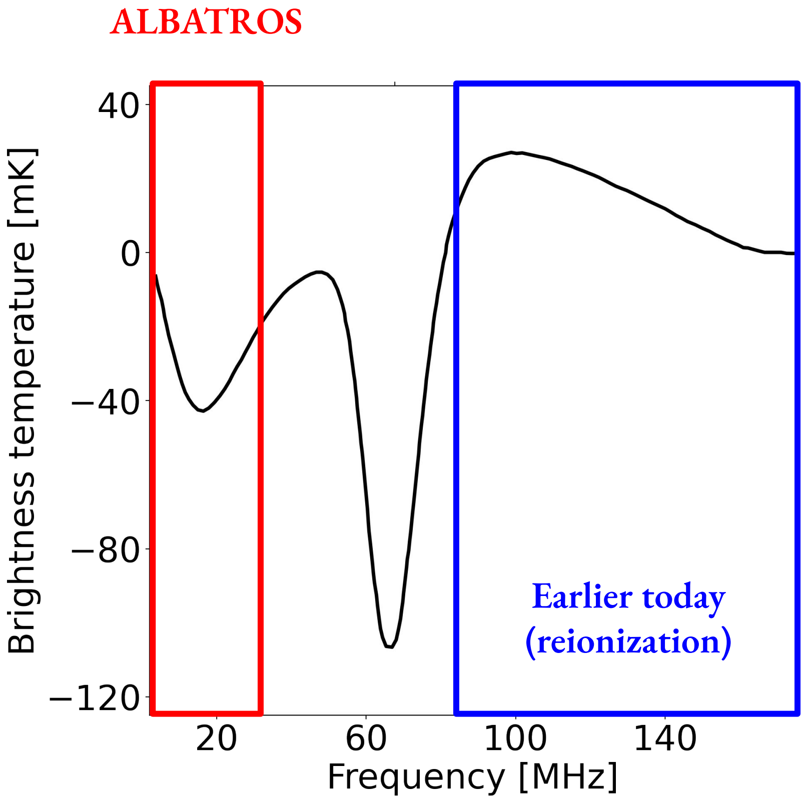

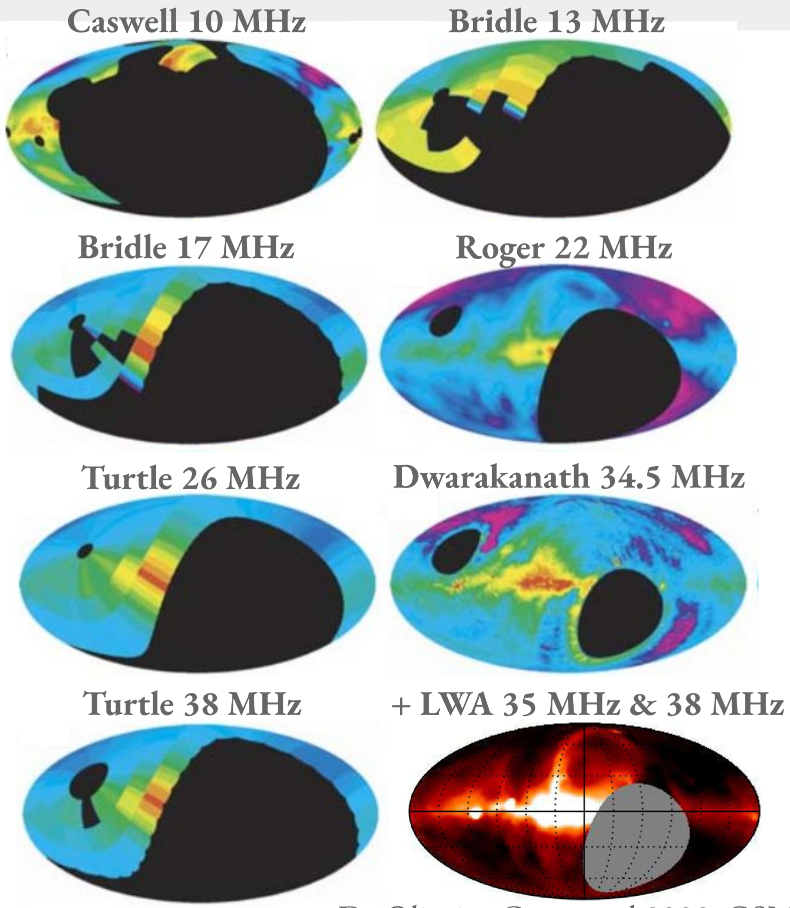

De Oliveira-Costa et al 2008, GSM

ALBATROS Overview

ALBATROS Synthesized beam at 5 MHz

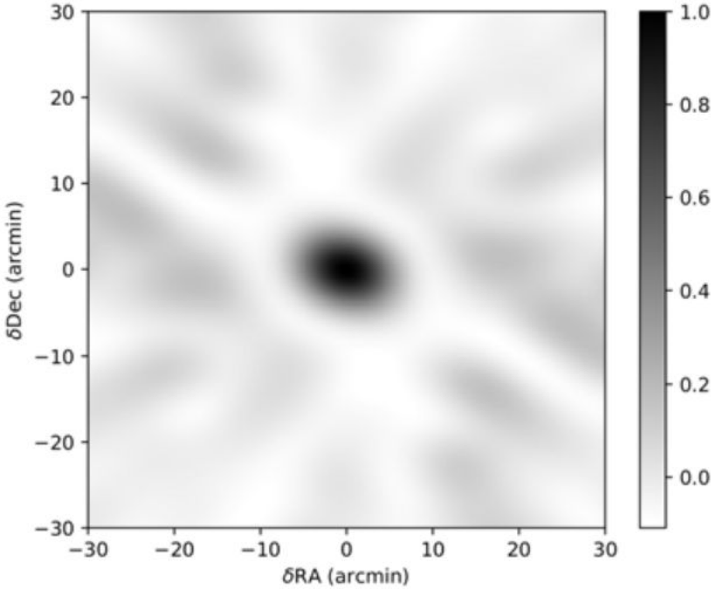

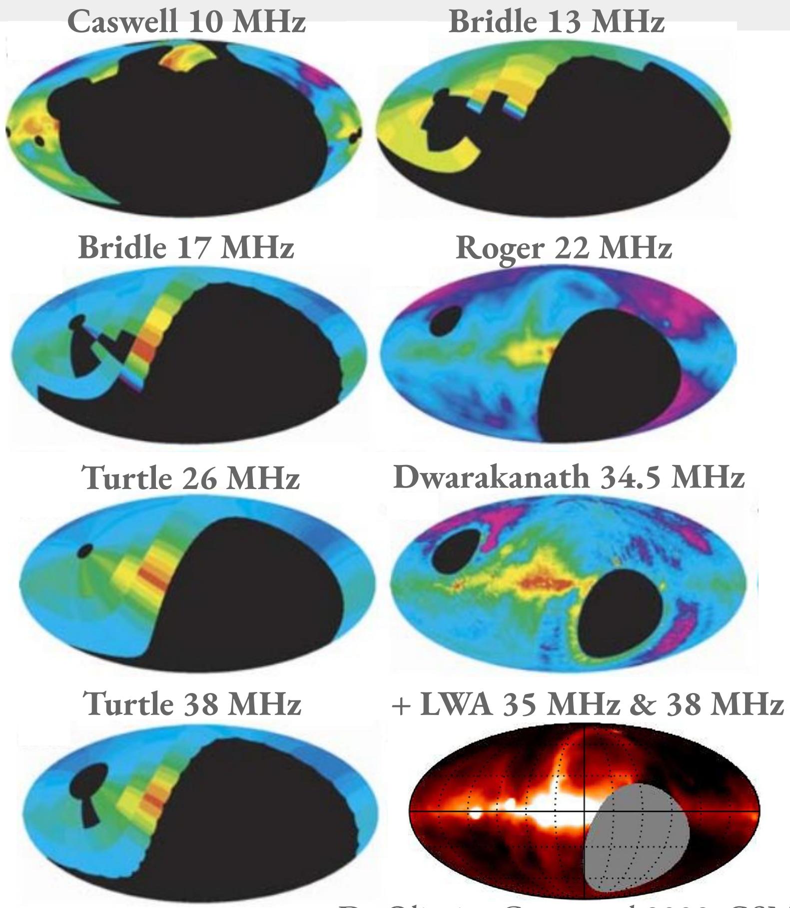

De Oliveira-Costa et al 2008, GSM

Simplified ALBATROS block diagram

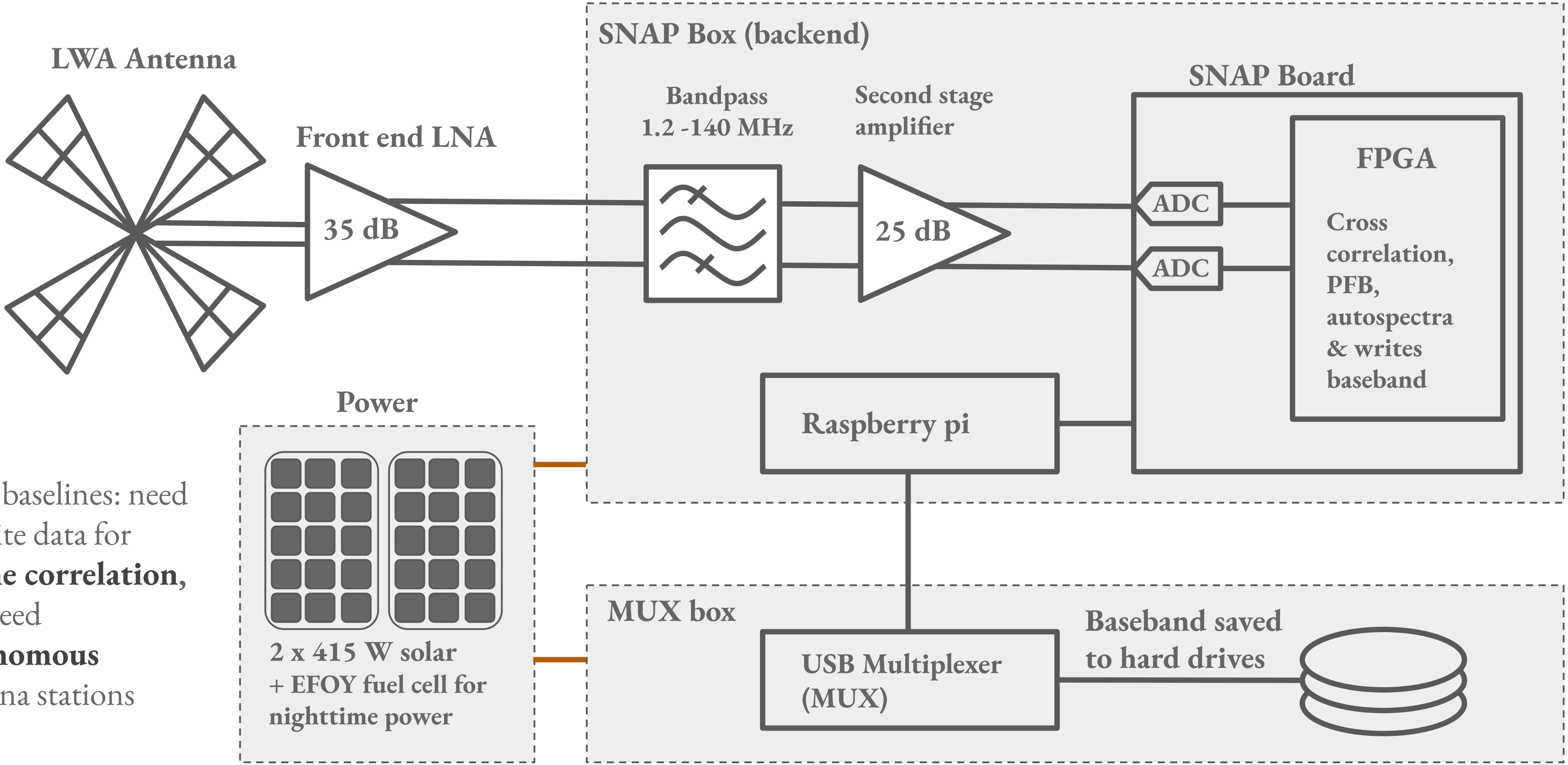

Long baselines: need to write data for **offline correlation,** and need **autonomous** antenna stations

Another requirement: **must** be low profile

Maxed out Twin Otter load
~20k CAD per Otter flight

Back-end and readout electronics

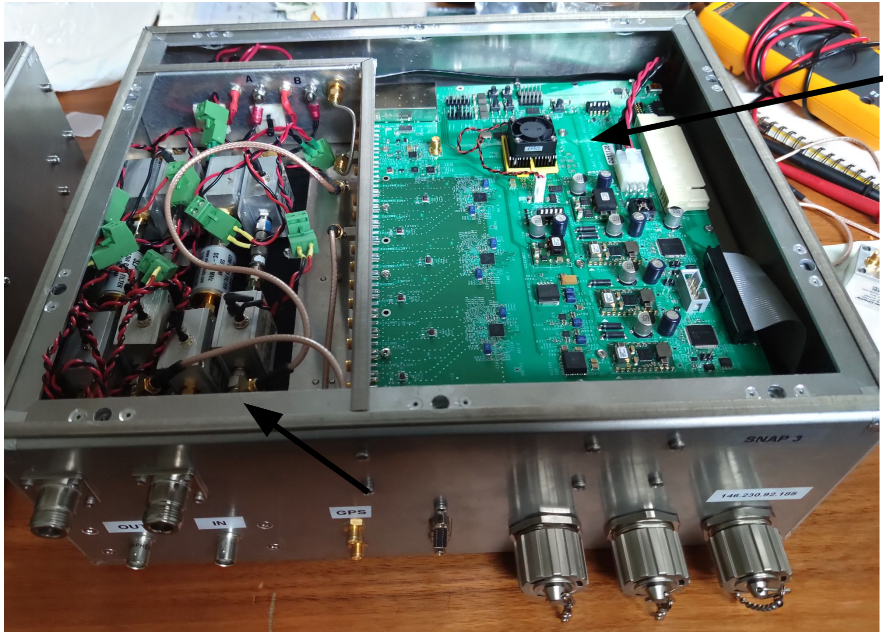

SNAP board:
0-125 MHz
250 msamples/s
2048 frequency channels (61 kHz)

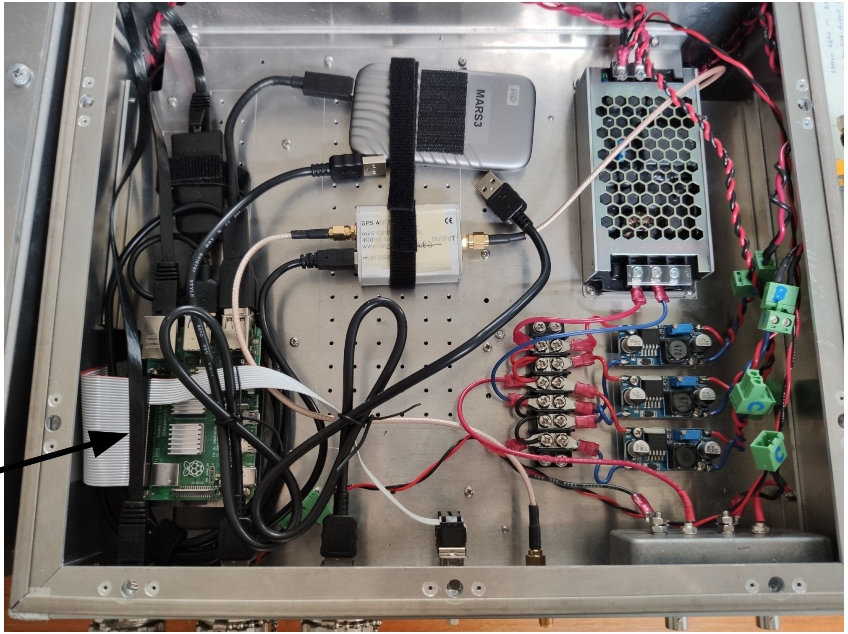

Raspberry Pi

Total system power draw ~ 45 W
Can easily fit in a backpack

Data storage

- Store 1 bit of baseband data for ~1 year of autonomous operation

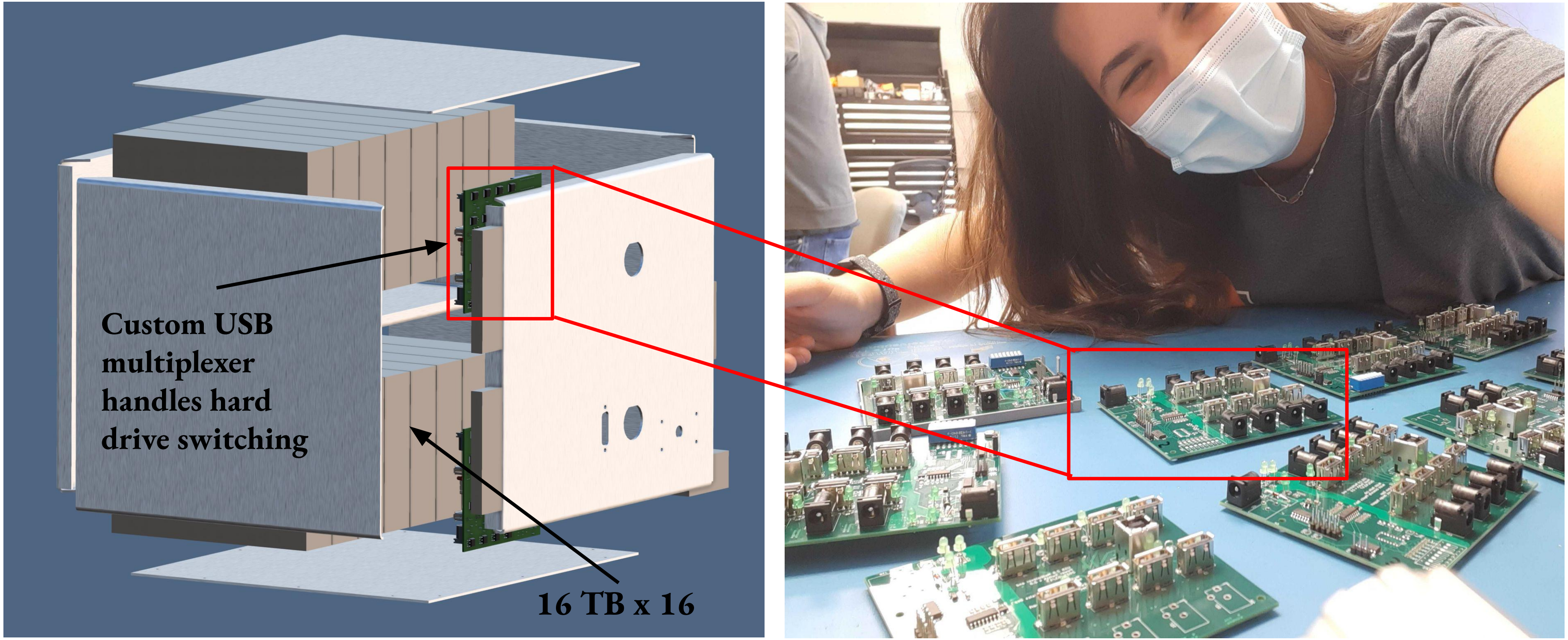

Power autonomy

Off the shelf hybrid solar and methanol generator (EFOY Pro Energy box)

Back-end electronics box

Hard drive box

Methanol tanks: 60L x 4

Front end amplifier and antenna response

- Currently using the long wavelength array (LWA) antenna and front end electronics: not optimized for these lowest frequencies.

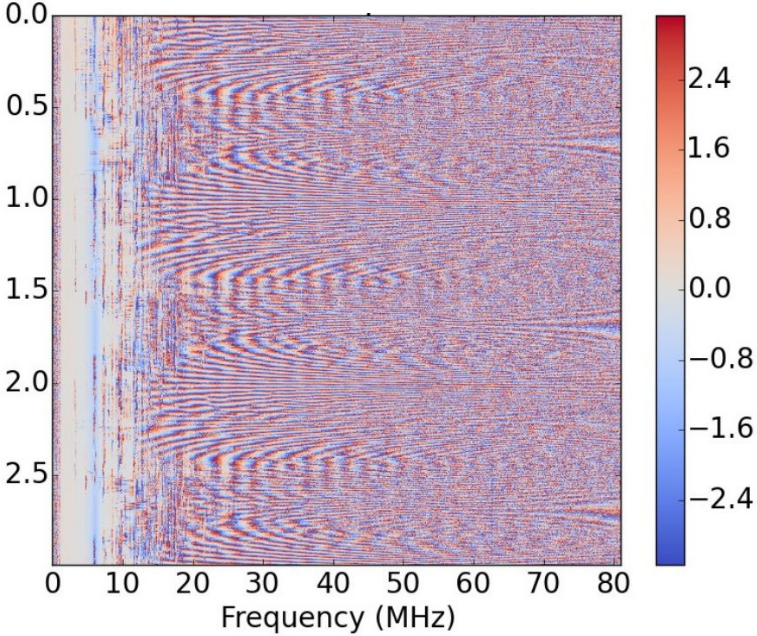

Cross spectra of 2-antenna pathfinder at Marion island (LWA)

Chiang et al 2020

Front-end electronics (FEE) development

- Custom high-impedance low-noise instrumentation amplifier

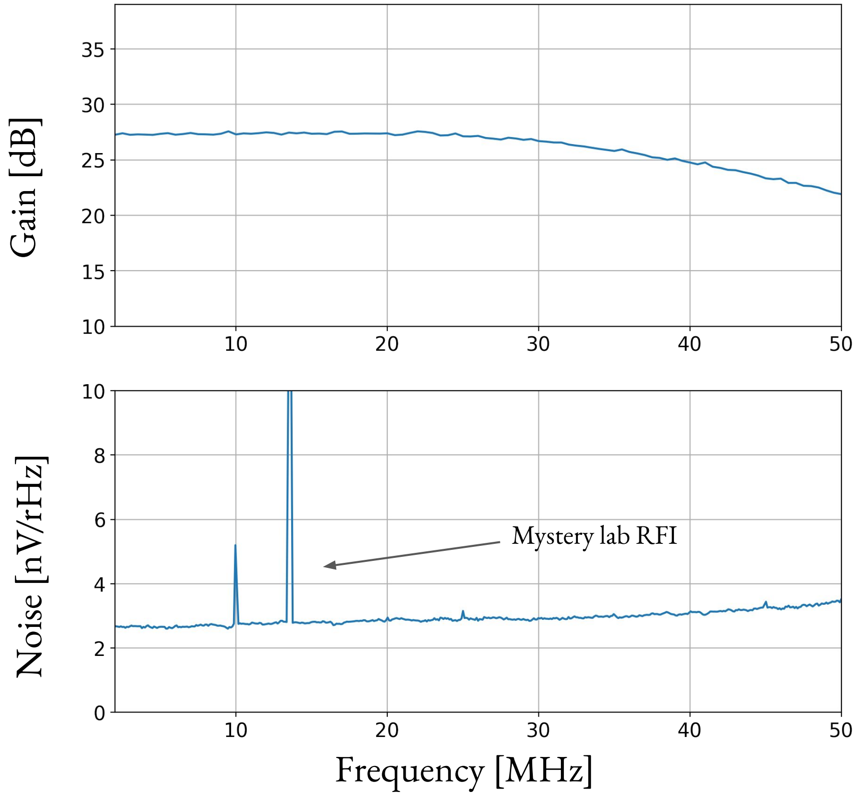

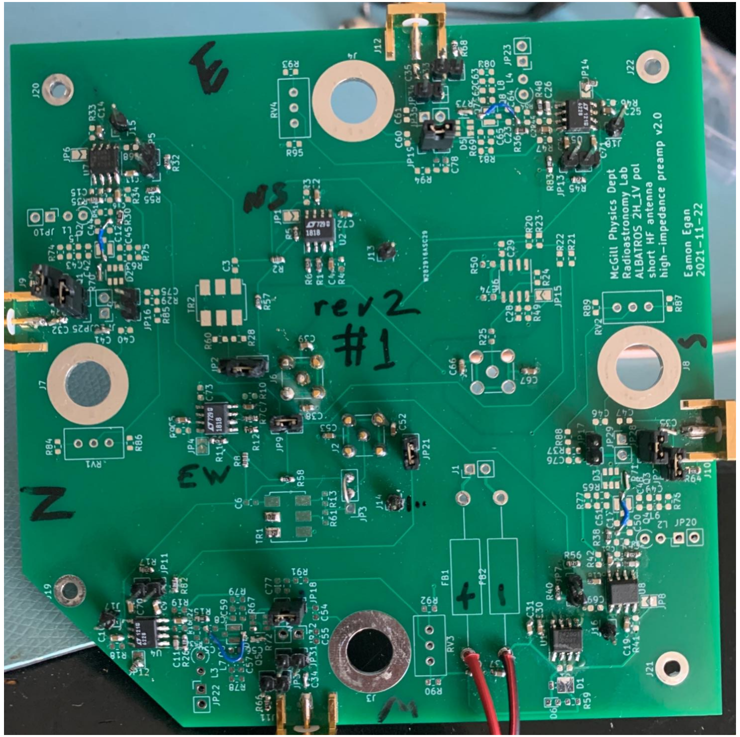

Team currently on site at Uapishka!

FEE proof of life: interferometric fringes

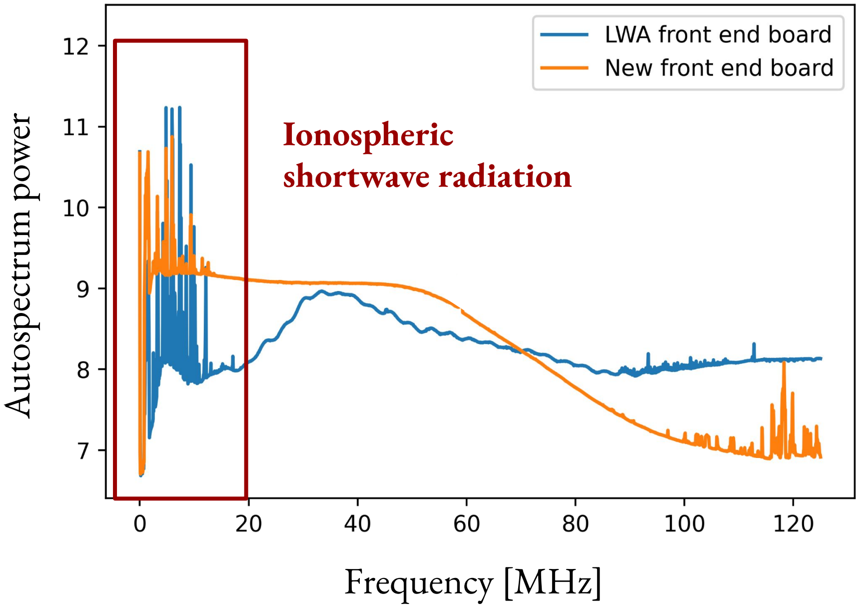

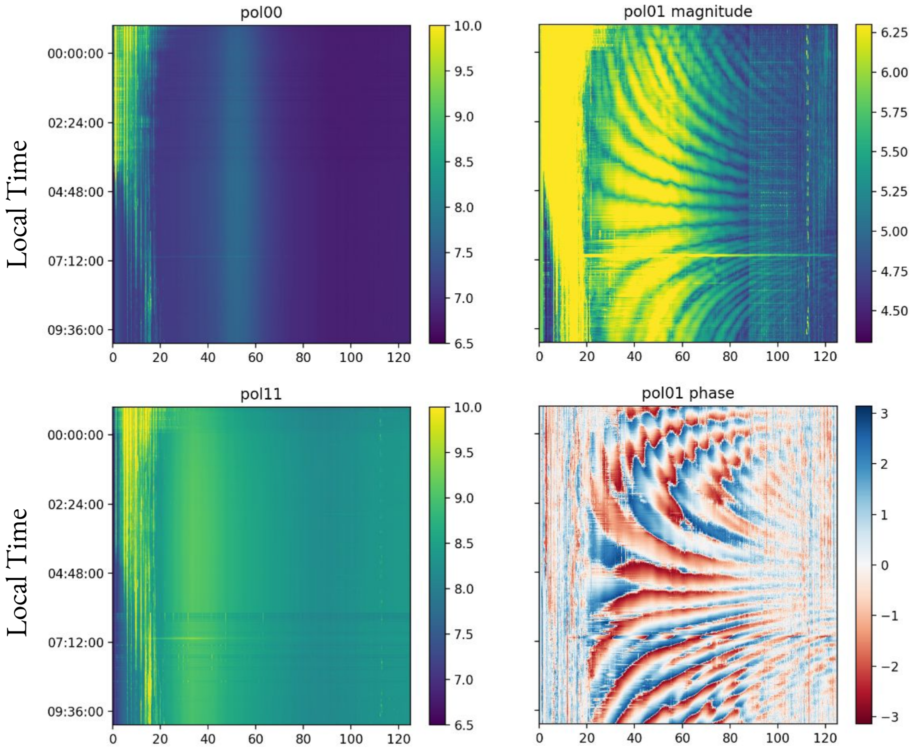

The McGill Arctic Research Station (MARS)

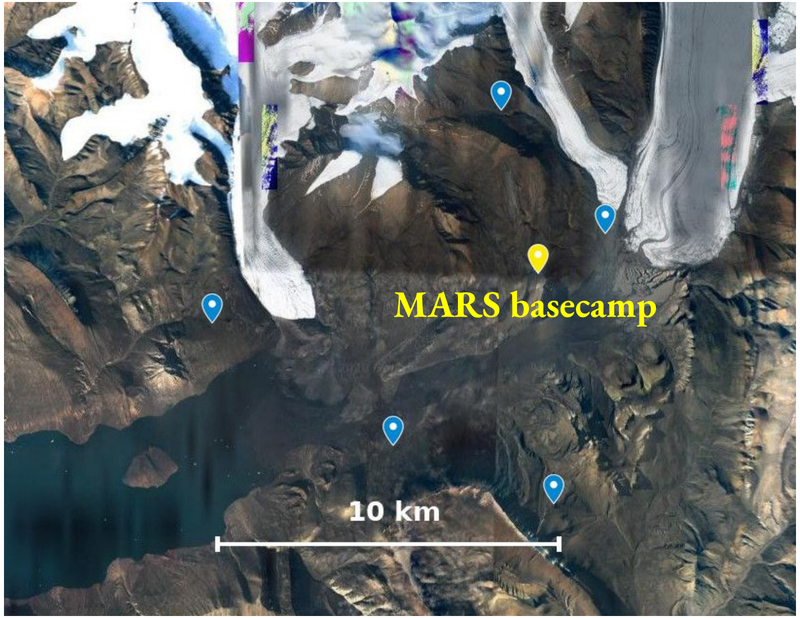

MARS basecamp


THE NORTH FACE


ALBATROS

Treacherous daily commute to work

Success for the 2022 field season! First Arctic baseline

Success for the 2022 field season! First Arctic baseline

Next steps for ALBATROS:

- 3 new antenna stations in the Arctic for 2023.
- Continued antenna and FEE development.
- Keep working on satellite timing for offline cross-correlation.
- Starlink to phone home?
- Drone beam mapping.

BACKUP SLIDES

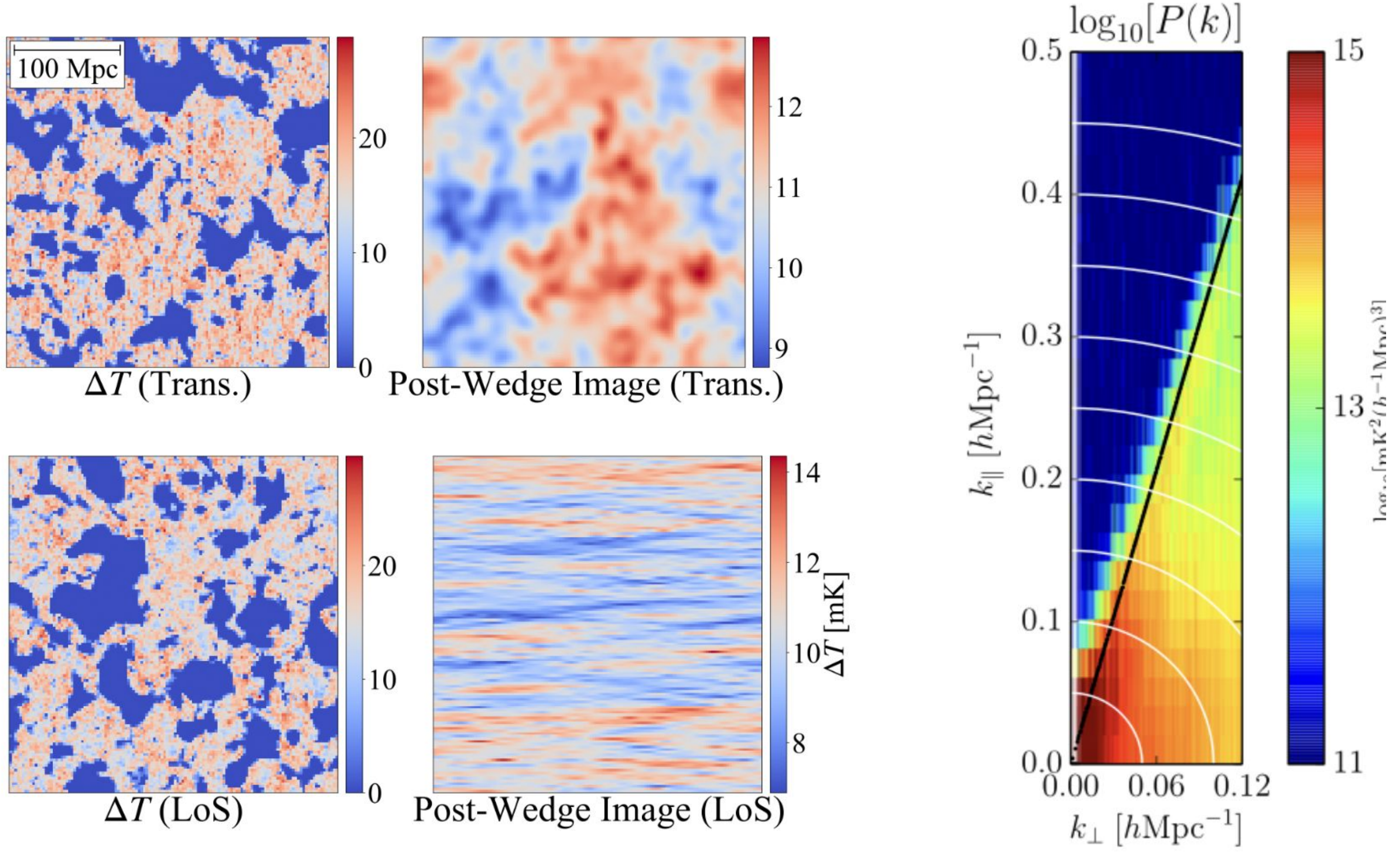

100 Mpc
ΔT (Trans.)
Post-Wedge Image (Trans.)
ΔT (LoS)
Post-Wedge Image (LoS)
ΔT [mK]
log10[P(k)]
k∥ [hMpc−1]
k⊥ [hMpc−1]
0.00
0.06
0.12
0.0
0.1
0.2
0.3
0.4
0.5
11
13
15
0
10
20
9
10
11
12
8
14

Simulating covariances: global 21cm signal

$$(\mathbf{C}^{21}_{\alpha\beta})^{-1} \approx \mathbf{F}^{21}_{\alpha\beta} = \sum_i \frac{\partial T_{21}(z_i)}{\partial x_{HI}(z_\alpha)} \mathbf{\Pi}_{\alpha\beta} \frac{\partial T_{21}(z_i)}{\partial x_{HI}(z_\beta)}$$

Approximated as analytic

$$\delta T_b \approx 27 x_{HI} \left(\frac{1+z}{10}\right)^{1/2} \text{mK}$$

$$(\mathbf{\Pi}_{\rm fg})_{\nu\nu'} = A^2 \left(\frac{\nu\nu'}{\nu_*^2}\right)^{-\alpha+\frac{1}{2}\Delta\alpha^2 \ln(\nu\nu'/\nu_*^2)} - m(\nu)\, m(\nu'), \quad (6)$$

with[1]

$$m(\nu) = A\left(\frac{\nu}{\nu_*}\right)^{-\alpha+\frac{1}{2}\Delta\alpha^2 \ln(\nu/\nu_*^2)}, \quad (7)$$

$$\sigma_i^2 = \frac{T^2_{\rm sky}(\nu_i)}{b\, t_{\rm int}},$$

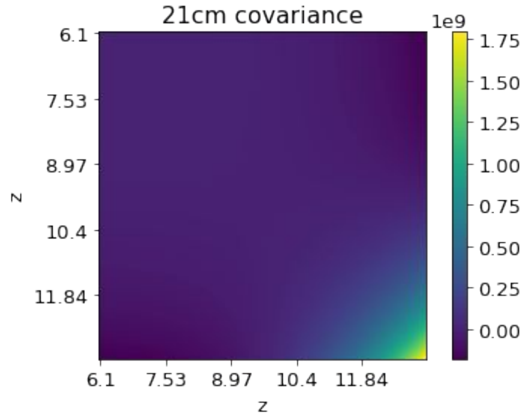

Instrument noise + foregrounds

Simulating covariances: kSZ

$$(\mathbf{C}^{kSZ}_{\alpha\beta})^{-1} \approx \mathbf{F}^{kSZ}_{\alpha\beta} = \sum_i \frac{\partial C_\ell(\ell_i)}{\partial x_{HI}(z_\alpha)} \mathbf{\Pi}_{\alpha\beta} \frac{\partial C_\ell(\ell_i)}{\partial x_{HI}(z_\beta)}$$

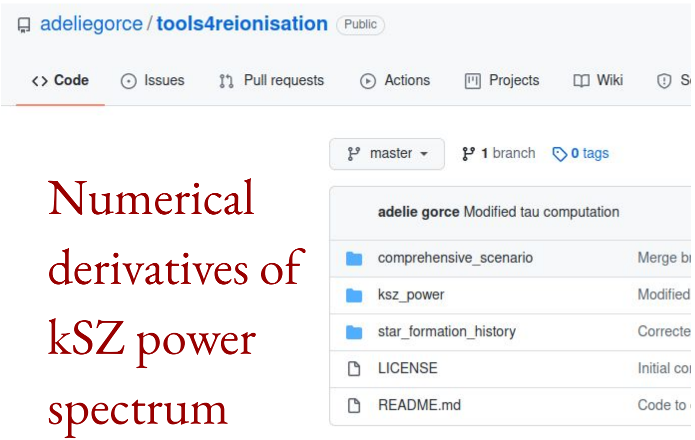

Numerical derivatives of kSZ power spectrum

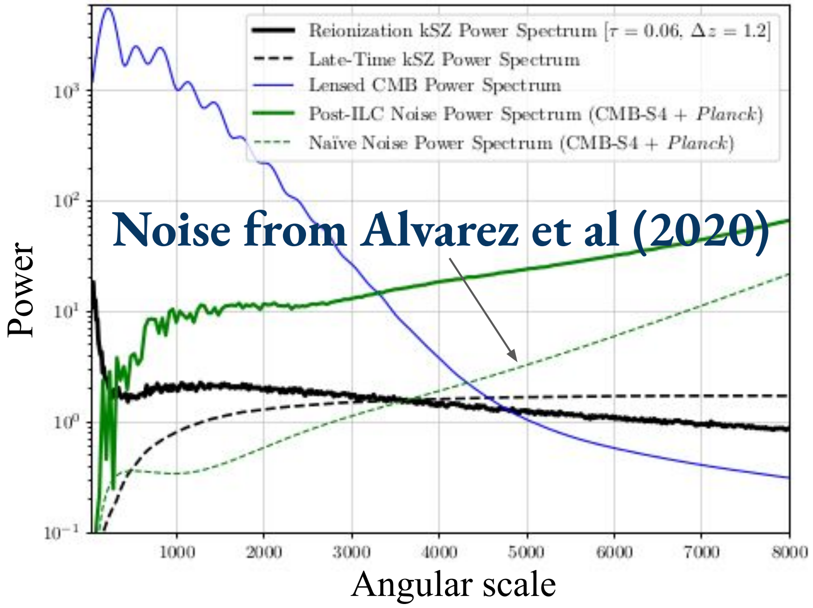

Noise from Alvarez et al (2020)

$$\mathbf{F}_{\mathrm{kSZ}}\mathbf{v} = \lambda \mathbf{F}_{21}\mathbf{v}, \tag{15}$$

where $\mathbf{F}_{\mathrm{kSZ}}$ and $\mathbf{F}_{21}$ are the Fisher matrices of the kSZ and 21cm global signal, respectively. Performing a Cholesky decomposition on the 21 cm covariance $\mathbf{C}_{21} = \mathbf{F}_{21}^{-1}$ allows us to write

$$\mathbf{F}_{21} = \mathbf{C}_{21}^{-1} = \mathbf{L}_{21}^{-T}\mathbf{L}_{21}^{-1}, \tag{16}$$

where $\mathbf{L}_{21}$ is a lower triangular matrix. Equation 15 then becomes

$$\mathbf{L}_{21}^{T}\mathbf{F}_{\mathrm{kSZ}}\mathbf{L}_{21}\mathbf{L}_{21}^{-1}\mathbf{v} = \lambda \mathbf{L}_{21}^{-1}\mathbf{v}, \tag{17}$$

which reduces to an eigenvalue problem

$$\mathbf{G}\mathbf{w} = \lambda \mathbf{w}, \tag{18}$$

with $\mathbf{G} \equiv \mathbf{L}_{21}^{T}\mathbf{F}_{\mathrm{kSZ}}\mathbf{L}_{21}$ and $\mathbf{w} \equiv \mathbf{L}_{21}^{-1}\mathbf{v}$. With these definitions, we define the KL transformation matrix as

$$\mathbf{R} \equiv \mathbf{L}_{21}\boldsymbol{\Psi}, \tag{19}$$

where the columns of $\boldsymbol{\Psi}$ are the eigenvectors $\mathbf{w}$ satisfying Equation (18). If we have a measurement of the ionization history $\mathbf{x} = (x_i(z_1), x_i(z_2), \ldots, x_i(z_n))$, its representation $\mathbf{y}$ in the KL basis is given by

$$\mathbf{y} = \mathbf{R}^{-1}\mathbf{x}, \tag{20}$$

and the inverse relation is

$$\mathbf{x} = \mathbf{R}\mathbf{y}. \tag{21}$$

In the KL basis, the information content (as expressed by the Fisher information matrices) is diagonal for both global 21 cm and kSZ measurements. Transforming their respective Fisher matrices via appropriate Jacobian factors, we obtain

$$\overline{\mathbf{F}}_{21} = \boldsymbol{\Psi}^{T}\mathbf{L}_{21}^{T}\mathbf{F}_{21}\mathbf{L}_{21}\boldsymbol{\Psi} = \boldsymbol{\Psi}^{T}\boldsymbol{\Psi} = \mathbf{I}, \tag{22}$$

for the 21 cm Fisher matrix in the KL basis and

$$\overline{\mathbf{F}}_{\mathrm{kSZ}} = \boldsymbol{\Psi}^{T}\mathbf{L}_{21}^{T}\mathbf{F}_{\mathrm{kSZ}}\mathbf{L}_{21}\boldsymbol{\Psi} = \boldsymbol{\Psi}^{T}\mathbf{G}\boldsymbol{\Psi} = \boldsymbol{\Lambda} \tag{23}$$

$$(\delta \mathbf{y}_{\mathrm{kSZ}})_\alpha = \sum_\gamma (\overline{\mathbf{F}}_{\mathrm{kSZ}}^{-1} \mathbf{R}^T)_{\alpha\gamma} \frac{\partial \mathbf{D}^T}{\partial x_i(z_\beta)} \mathbf{\Pi}_{\mathrm{kSZ}}^{-1} \delta \mathbf{D}. \tag{43}$$

To simulate the CMB primary contaminating our kSZ measurement, we take $\delta\mathbf{D}$ to be a scaled primary CMB power spectrum. We allow the residual primary CMB temperature at $\ell = 3000$, $\delta D^{\mathrm{CMB}}_{\ell=3000}$, to range up to $0.3\,\mu\mathrm{K}^2$ and find that even for small primary CMB residuals, $\mathbf{z}$ is perturbed well outside the error bars for the overlap modes. This is unsurprising due to the large dynamic range of the CMB power spectrum over the range of ℓ that we are considering. Although a CMB temperature of $1\,\mu\mathrm{K}^2$ at $\ell = 3000$ is of the same order as the kSZ signal at this ℓ, the CMB can be up to two orders of magnitude brighter on the lower end of our ℓ range.

$$\nu \equiv \frac{|\mathbf{s}^T \mathbf{\Sigma}^{-1} \mathbf{z}|}{\sqrt{\mathbf{s}^T \mathbf{\Sigma}^{-1} \mathbf{s}}}.$$